Chapter 14
Decoration of Inorganic Substrates with Metallic Nanoparticles and Their Application as Antimicrobial Agents

Marianna Hundáková, Kateřina Dědková, and Gražyna Simha Martynková

Abstract Effect on antimicrobial activity observed for several types of hybrid materials is described in our chapter. The substrates for functional antimicrobial particles are natural clay minerals and carbon materials for this review limited to graphite/graphene and carbon nanoparticles (nanotubes and fullerenes). Short description of substrate materials and their properties is followed by discussion of the effect of selected most popular antimicrobial metals (silver, copper) and several oxides (zinc, titanium and copper oxides) and it is conferred for Gram positive and Gram negative bacterial strains. The methods for preparation of such particles may vary but the most used are intercalation and decoration methods from solution for the clay minerals. Nanoparticles (NPs) of metals and metal oxides on carbon and nanocarbon materials are prepared using physico-chemical approach. The research confirmed that the shape and size of functional NPs can depend on used substrate, preparation conditions and used method. Interestingly, it was found that Ag-clay sample was as effective as the free Ag+ions. Generally, it was found the size of active surface area, mobility and availability of potential active particles (ions or nanoparticles) and chemical state of them plays an important role in antimicrobial activity.

Keywords Antimicrobial activity • Silver • Copper • Zinc oxide • Titanium oxide • Nanoparticles • Clay minerals • Carbon materials

M. Hundáková • K. Dědková (✉)
Nanotechnology Centre, VŠB-Technical University of Ostrava,
17.listopadu 15/2172, 70833 Ostrava, Poruba, Czech Republic

Regional Materials Science and Technology Centre, VŠB-Technical University of Ostrava,
17. listopadu 15/2172, 70833 Ostrava, Poruba, Czech Republic
e-mail: katerina.dedkova@vsb.cz

G.S. Martynková
Nanotechnology Centre, VŠB-Technical University of Ostrava,
17.listopadu 15/2172, 70833 Ostrava, Poruba, Czech Republic

M. Rai, R. Shegokar (eds.), *Metal Nanoparticles in Pharma*,
DOI 10.1007/978-3-319-63790-7_14

14.1 Introduction

The word antimicrobial was derived from three the Greek words anti (against), mikros (little) and bios (life) and refers to all agents that turn against microbial organisms. This is not synonymous with antibiotics, a similar term derived from the Greek word anti (against) and biotikos (concerning life). By strict definition, the word "antibiotic" refers to substances formed by microorganisms that act against another microorganism. Thus, antibiotics do not include antimicrobial substances that are synthetic (sulfonamides and quinolones), or semisynthetic (methicillin and amoxicillin), or those which come from plants (quercetin and alkaloids) or animals (lysozyme). In contrast, the term "antimicrobials" include all agents that turn against all types of microorganisms - bacteria (antibacterial), viruses (antiviral), fungi (antifungal) and protozoa (antiprotozoal).

Antimicrobials are classified in several ways, as: spectrum of activity, effect on bacteria, mode of action or as the basic (cationic), the uncharged (neutral) and the acidic (anionic groups). Antimicrobials often display different minimum inhibition concentration (MIC) values, especially between Gram-negative (G^-) and Gram-positive (G^+) bacteria strains. The G^- strains are less susceptible to antibiotics due to the permeability barrier provided by their outer membrane. Consequently, a full characterization of antibacterial activity should be assessed using both types of organisms. Examples of commonly found G^- bacteria are *Escherichia coli, Salmonella typhimurium* and *Pseudomonas aeruginosa*, and examples of G^+ strains are *Streptococcus aureus* and *Streptococcus pyogenes*.

There is interest to expand of range of antimicrobial agents for other than most popular silver, since extensive and uncontrolled use of silver, is increasing public interest to address and monitor the clinical risk related to silver resistance and in an environmental context to study the sources, fate, transport routes and toxicity of environmentally relevant forms of silver. Over the past few years, various nano-sized antibacterial agents such as metal and metal oxide nanoparticles have been evaluated by researchers. Several types of metal and metal oxide nanoparticles apart from silver (Ag) and silver oxide (Ag_2O), the titanium dioxide (TiO_2), zinc oxide (ZnO), gold (Au), copper oxide (CuO), and magnesium oxide (MgO) have been known to show antimicrobial activity (Jakobsen et al. 2011; Vargas-Reus et al. 2012).

Silver and copper belongs to the metals, which are by tradition known their antibacterial behavior. In last years, silver compounds are studied as antimicrobial agents for many applications, for example, as silver-coated endotracheal tubes to reduce incidence of ventilator-associated pneumonia (Kollef et al. 2008) as a safe preservative for use in cosmetics Kokura et al. 2010, as additive to water based paints (Holtz et al. 2012), in textiles (Üreyen et al. 2012) and other applications (Rai et al. 2009). Copper compounds are studied as antimicrobial agents, for example, for drinking water treatment (Dankovich and Smith 2014) and for other applications (Vincent et al. 2016).

The mechanism of the antimicrobial action of metal nanoparticles (NPs) is not fully understood. Some authors described possible action and interaction of metals

with the bacterial cell. The antibacterial tests showed the differences in antibacterial action of materials containing Ag between the G+ and the G- bacteria. This can be explained by differences in structure of bacterial cell. While the cell wall of the G+ bacteria consists of a thick layer of peptidoglycan with lipoteichoic acid or another acidic polymer, the cell wall of G- bacteria is formed by lipopolysaccharides and phospholipids and only a thin layer of peptidoglycan. The thick layer of peptidoglycan can make bacteria more resistant before the metal ions and NPs (Russell 2001; Zhao et al. 2006). It was observed and confirmed that several actions take place during interaction of the Ag+ ions with bacteria: (1) the Ag+ ions penetrate during the cell wall into the bacteria cell, where (2) interact with thiol groups in proteins and caused their inactivation, and moreover, (3) the Ag+ in the bacteria cell caused that DNA molecules become condensed and lose their replication abilities (Feng et al. 2000).

In case of Ag NPs, the size of NPs play important role in antimicrobial action. It was observed that smaller particles exhibited higher antimicrobial activity (Panáček et al. 2006). The small Ag NPs were incorporated into the membrane structure. The treated bacteria cell showed changes and damage to membrane which leads to increase in their permeability. The bacterial cells incapable of properly regulating transport through the plasma membrane; the cytoplasmic content is released to the medium which is causing cell death without affecting proteins or nucleic acids (Sondi and Salopek-Sondi 2004; Rai and Bai 2011). Large specific surface area of NPs can influence the antimicrobial action as well. The antibacterial properties of Ag NPs are related to the total surface area of the NPs. Smaller particles with a larger surface to volume ratio are more efficient agents for antibacterial activity (Baker et al. 2005).

The proteomic analysis of Ag NPs on *E. coli* shows that the Ag NPs destabilized the outer membrane and disrupts the outer membrane barrier components. The mode of action Ag NPs was found to be like that of Ag^+ ions. However, the effective concentrations of Ag NPs and Ag^+ ions were found to be at nanomolar and micromolar levels, respectively (Lok et al. 2006).

The mechanism of the bacteria cells inhibition by Cu^{2+} ions and CuO or Cu_2O NPs work in a similar way as silver agents. The G^- bacteria with an outer membrane covering a thin layer of peptidoglycan which is negatively charged probably binds the Cu^{2+} ions. Both G^+ and G^- strains turned from normal rod-shape into irregular shape (round, ellipse, etc.) after treatment with Cu-montmorillonite. The cell wall was destroyed, bacterial inner vacuoles appeared, there was an efflux of nutrient, the space between the cell wall and cell membrane widened, and the cytoplasm tended to concentrate. The Cu^{2+} can combine with the plasma membrane by electrostatic attraction and penetrate into the cell membrane through opening or closing of the membrane channel. This affects the permeability of cellular membranes and results in leakage of intracellular ions and low molecular-weight metabolites. Moreover, the Cu^{2+} enters into the cell strongly combines with intracellular sulfur-containing amino acids, which leads to denaturation of protein and bacterial death (Tong et al. 2005). The CuO or Cu_2O NPs caused bacterial membrane damage. The NPs due to the appropriate charge and small size can penetrate the membrane and

cause bacteria cell death by the production of reactive oxygen species or by the disruption of cell function thereby affecting proteins and DNA (Meghana et al. 2015).

Titanium dioxide (TiO_2) is known for its chemical stability, photocatalytic characteristics, durability and antimicrobial activity, which could be attributed to its crystal structure (Chung et al. 2009). Anatase has stronger antimicrobial and photocatalytic activity than rutile (Chung et al. 2007a, b, 2011). Titanium dioxide is known for reactive oxygen species (ROS) production via photoactivation due to UV-light. There are also studies which find ROS production in the absence of photoactivation (Gurr et al. 2005). TiO_2 can promote the decomposition of inorganic and organic compounds, which could be used in potential applications in sanitation and sterilization. Materials coated with TiO_2 are already being used as antibacterial materials (Hashimoto et al. 2005).

Among metal oxide powders, *ZnO* demonstrates significant growth inhibition of broad spectrum of bacteria (Jones et al. 2008). The suggested mechanism for the antibacterial activity of ZnO is based on catalysis of formation of reactive oxygen species (ROS) (Yamamoto et al. 2002). Since the catalysis of radical formation occurs on the particle surface, particles with larger surface area demonstrate stronger antibacterial activity. Therefore, as the size of the ZnO particles decreases their antibacterial activity increases (Jones et al. 2008).

Nevertheless, metal ions and NPs could also be toxic for living organisms mainly at higher concentrations (Braydich-Stolle et al. 2005; Lu et al. 2010; Chang et al. 2012). Therefore, it is desirable to control their gradual release. For this purpose metal ions or metal NPs and their oxides may be prepared anchored on various inorganic substrates. The most commonly used substrates include clay minerals, zeolites or carbon materials.

Clay minerals are widely used as supports for metals or metal oxides preparation. Clay minerals belong to the layered silicates (phyllosilicates) with structure consist from octahedral and tetrahedral sheets. Based on the sheets arrangement to the layers, clay minerals are divided to the two groups, with type of layer 1:1 and 2:1. The 1:1 type consists of the repetition of one tetrahedral sheet and one octahedral sheet. The 2:1 type consists of the repetition of one octahedral sheet sandwiched between two tetrahedral sheets. The composition of the 1:1 phyllosilicates is characterized by a predominance of Al^{3+} as central octahedral cations, although some isomorphous substitution of Mg^{2+}, Fe^{3+}, Ti^{4+} for Al^{3+} can occur. The composition of the 2:1 phyllosilicates is characterized by a predominance of Si^{4+} as central octahedral cations and Al^{3+} and Fe^{3+} as central tetrahedral cations. Central cations are usually substituted by cations with lower valance as Al^{3+}, Fe^{3+}, Fe^{2+}, Mg^{2+}, etc. and a negative charge arising on layers from these substitutions. The charge variability is one of the most important features of 2:1 phyllosilicates, because it induces occupancy of the interlayer space by exchangeable cations which compensate the negative layer charge. Due to the low proportion of substitution in 1:1 phyllosilicates the layer charge is usually close to zero, so the interlayer space is without exchangeable cations (Brigatti et al. 2006). To the 1:1 phyllosilicates using as supports for metal nanoparticles preparation belong, for example, kaolinite (Kao)

and halloysite (Hal) and to the 2:1 phyllosilicates belong montmorillonite (Mt), vermiculite (Ver), talc, palygorskite (Pal) and sepiolite (Sep).

Mt is defined as dioctahedral smectite. Smectites are swelling and turbostratically disordered minerals occurring in nature as the main component of bentonites. The term smectite is used for planar dioctahedral and trioctahedral 2:1 clay minerals with a layer charge between −0.2 and −0.6 per formula unit which contain hydrated exchangeable cations. Minerals of the smectite group have high specific surface area and ability of cation exchange capacity. Hydrated exchangeable cations between the layers compensate the negative charge and may be easily exchanged by other metal cations. The cation exchange capacity (CEC) is the measure of the cations, which balance the negative charge sites of the clay (Valášková and Martynkova 2012). Ver is planar dioctahedral and trioctahedral 2:1 clay mineral with a layer charge between −0.6 and −0.9 per formula unit which contain hydrated exchangeable cations. Hal is a 1:1 layered aluminosilicate structure chemically similar to Kao. The size of Hal tubules varies within 0.5–10 microns in length and 15–200 nm in inner diameter, depending on the deposit. Pal structure of 2:1 layers consists of the continuous two-dimensional tetrahedral sheet but lacking continuous octahedral sheet. Pal is characterized by microfibrous morphology, low surface charge and high surface area (Martynková and Valášková 2014).

Other groups of minerals are zeolites. Zeolites (Zeol) belong to the hydrated aluminosilicates with three-dimensional structures with independent component: the alumunosilicate framework, exchangeable cations and zeolitic water. The Zeol framework is composed from tetrahedron, which center is occupied by Si^{4+} or Al^{3+} cations, with four oxygen atoms at the vehicles. Due to the substitution of Si^{4+} by Al^{3+} arise the negative charge on the framework, which is compensated by cations located together with water. The water molecules can be in large cavities and bonded between framework and exchangeable ions. The most common representative of Zeol is clinoptilotite (Cli) (Wang and Peng 2010).

Health and environmental impacts of *graphene-based materials* need to be thoroughly evaluated before their potential applications. Graphene has strong cytotoxicity toward bacteria. To better understand its antimicrobial mechanism, comparison of the antibacterial activity of four types of graphene-based materials (graphite (Gt), graphite oxide (GtO), graphene oxide (GO), and reduced graphene oxide (rGO)) toward a bacterial model – *Escherichia coli* is given. GO dispersion shows the highest antibacterial activity, sequentially followed by rGO, Gt, and GtO. The direct contacts with graphene nanosheets disrupt cell membrane. Conductive rGO and Gt have higher oxidation capacities than insulating GO and GtO. Antimicrobial actions are contributed by both membrane and oxidation stress. Physicochemical properties of graphene-based materials, such as density of functional groups, size, and conductivity, can be precisely tailored to either reducing their health and environmental risks or increasing their application potentials (Liu et al. 2011).

The ability of carbon nanotubes (CNTs) to undergo surface modification allows them to form advanced nanocomposites with different materials such as polymers, metal nanoparticles, biomolecules, and metal oxides. The biocidal nature, protein fouling resistance, and fouling release properties of CNT-NCs render them the per-

fect material for biofouling prevention (Narayan et al. 2005). Cytotoxicity of CNT can be reduced before applying them as substrates to promote biofilm formation in environmental biotechnology applications.

To understand the inherent antimicrobial nature of pristine CNTs is key issue that may determine the efficiency of biocidal CNT-nanocomposites. Microorganisms lose viability when they come in contact with nanotubes; due to the impingement of nanometer-sized fibers and the needle-like character of CNTs easily penetrate through the cell walls of bacteria (Narayan et al. 2005). CNTs in solution develop nanotube networks on the cell surface, and then destroy the bacterial envelopes with leakage of the intracellular contents (Liu et al. 2010). The antimicrobial effect of CNTs has been demonstrated over a wide range of microorganisms including bacteria provided confirmatory evidence that both, single wall carbon nanotubes (SWCNTs) and multiwall carbon nanotubes (MWCNTs) are able to decrease the metabolic activity of *E. coli*. SWCNTs can produce cytotoxic effects on microbial communities in macro-environmental entities. Efficient contact between the CNTs and bacterial cell surface is crucial the biocidal action of CNTs. However, this effort depends on a variety of factors, such as: (i) physical and structural properties of CNTs (size and length); (ii) physical condition of CNTs (aggregated or dispersed); (iii) type and concentration of impurities associated with CNTs and their availability to bacteria (heavy metal impurities); and (iv) number of layers (single or multiwalled) of CNTs (Martynková and Valášková 2014). Normally, loosely packed, debundled, highly dispersed, and shorter length tubes can easily penetrate through the cell membrane and display higher cell cytotoxicity.

Fullerenes are soccer ball-shaped molecules composed of carbon atoms. Fullerenes showed antimicrobial activity against various bacteria. The antibacterial effect was probably due to inhibition of energy metabolism after internalization of the nanoparticles into the bacteria (Shvedova et al. 2012). It has also been suggested that fullerene derivatives can inhibit bacterial growth by impairing the respiratory chain (Cataldo and Da Ros 2008; Deryabin et al. 2014). In the beginning, a decrease of oxygen uptake (at low fullerene derivative concentration) and then an increase of oxygen uptake (followed by an enhancement of hydrogen peroxide production) are occurred. Another bactericidal mechanism, which has been proposed, was the induction of cell membrane disruption. Hydrophobic surface of the fullerenes can easily interact with membrane lipids and intercalate into them. The discovery of fullerenes ability to interact with biological membranes has encouraged many researchers to evaluate their antimicrobials applications (Tegos et al. 2005; Yang et al. 2014).

The cationic-substituted fullerene derivatives are highly effective in killing a broad spectrum of microbial cells after irradiation with white light. Affecting factor was an increased number of quaternary cationic groups that were widely dispersed around the fullerene cage to minimize aggregation. The quaternized fullerenes could be effectively applied in treatment of superficial infections, e.g. wounds and burns, where light penetration into tissue is not problematic (Mizuno et al. 2011).

Nowadays, many publications are focused on the preparation, characterization and study of the functional properties (especially catalytic) of silver, copper, zinc and titanium oxide nanoparticles on inorganic substrates. In this chapter, we focus only on the research that describes study of antimicrobial properties of these materials.

14.2 Metals on Inorganic Substrates as Antimicrobial Agent

14.2.1 Silver on Clay Minerals

Silver can be synthesized on inorganic substrates via several methods: as Ag^+ ions and Ag or Ag_2CO_3 NPs. Summary of selected preparation techniques of Ag on the various substrates, tested bacterial strains and methods used for studying the antimicrobial activity is shown in Table 14.1.

Montmorillonite is widely used clay mineral for various industrial and medical applications. Antibacterial properties of Ag modified Mt on Gram-negative (G^-) bacterium *Escherichia coli (E. coli)* were studied. Mt was pretreated by calcination at 550 °C or by grinding, followed by enriching with Ag using cation exchange methods. The metallic Ag^0 NPs precipitated on clay surface was confirmed. Nevertheless, the Ag^+ ions were also incorporated in the interlayer of Mt structure. Results of antibacterial activity of Ag-Mt composites, evaluated via the disc susceptibility (DS) test and by determination of the minimum inhibitory concentration (MIC) test, showed good inhibition properties on the growth of *E. coli*. The antibacterial behavior was affected by the availability of the ionic Ag^+ to be in contact with the bacteria (Magaña et al. 2008).

The simple preparation process of Ag NPs on Mt matrix included the stirring of Mt with $AgNO_3$ aqueous solution at room temperature. The mean particle size of Ag NPs on Mt surface was 50 nm and more on the edges of the Mt flakes. Antibacterial activity was tested via the broth dilution method by MIC value determination. The Gram-positive (G^+) bacteria *Staphylococcus aureus* (*S. aureus*) and *Enterococcus faecalis* (*E. faecalis*) and the Gram-negative (G^-) bacteria *Klebsiella pneumoniae* (*K. pneumoniae*) and *Pseudomonas aeruginosa* (*P. aeruginosa*) were used for antibacterial test. Antibacterial action of samples started after 1.5 h against the G^- bacteria and after 3–5 h against the G^+ bacteria and action was persisting for the whole testing period 6 days. Moreover, authors studied release of Ag^+ from Mt matrix into the water environment, which was determined as 0.1–0.3% from the total Ag content in the samples (Valášková et al. 2010). Antibacterial study of the Ag^+- exchanged and Ag^0- covered Mt samples showed good inhibition effect determined by the disk diffusion method against bacteria *P. aeruginosa* (G^-) and *S. aureus* (G^+). The diameter of inhibition zone was in the range 20–21 and 21–22 mm for Ag^+-Mt and Ag^0-Mt, respectively (Özdemir et al. 2010). The antibacterial and antifungal properties of Ag-Mt prepared by cation exchange method on Mt using $AgNO_3$ aqueous solution

Table 14.1 Summary of methods and precursors used for the preparation of silver on the inorganic substrates, used testing methods, and bacterial strains for studying the antimicrobial activity of prepared materials

Method, precursor (conditions)	Inorganic substrate, chemical pretreatment	Tested bacteria	Testing method, test evaluation	Reference
Stirring, $AgNO_3$ (room temperature, 1 week)	Mt (Pellegrini Lake, Argentina) – pretreated by (a) calcination, (b) grinding	*E. coli*	Disk susceptibility test, MIC determination	Magaña et al. (2008)
Shaking, $AgNO_3$ (room temperature, 24 h)	Mt (Ivančice, Czech Republic), Ver (China)	*S. aureus*, *P. aeruginosa*, *K. pneumoniae*, *E. faecalis*	Broth dilution method, MIC determination	Valášková et al. (2010)
Shaking, $AgNO_3$, $Cu(NO_3)_2$, $Zn(NO_3)_2$, CP (room temperature, 24 h)	Mt (Middle Anatolia) – purified	*S. aureus*, *P. aeruginosa*	Disk diffusion method	Özdemir et al. (2010)
Shaking, $AgNO_3$, $ZnSO_4$, $CuSO_4$ (room temperature, 24 h)	Na^+-rich Mt (SWy2) (Crook County, Wyoming)	*E. coli*, *P. cinnabarinus*, *P. ostreatus*	CFU counting, median effective concentration (EC50)	Malachová et al. (2011)
Melting, $AgNO_3$, $NaNO_3$ (435 °C, 4h)	Ben (San Juan, Mexico) – pretreated with acid (HCl or H_2SO_4)	*E. coli*, *S. aureus*	Agar diffusion method, MIC determination	Santos et al. (2011)
(1) Ion exchange, Ag_2O, $NH_3{\cdot}H_2O$ (60 °C, 4 h), (2) UV-photoreduction (PVP, high pressure mercury lamp)	Mt (from Zhejiang Fenghong Clay Chemicals Corp., China)	*E. coli*	Broth microdilution method, MIC determination, sterilizing efficiency	Xu et al. (2011)
Cation exchange, $AgNO_3$ – use in suture	Mt (from Sanding Technology Company in Zhejiang Province, China) – purified	*E. coli*, *S. aureus*	CFU counting, hemolysis test, in vitro cytotoxicity test	Cao et al. (2014)
(1) Shaking, $AgNO_3$ (room temperature, 24 h), (2) reduction, $NaBH_4$ (shaken, several min, room temperature)	Na^+-rich Mt (SWy2) (Crook County, Wyoming)	*E. coli*, *E. faecium*	MIC determination	Malachová et al. (2009)
(1) Absorption, $AgNO_3$, n-hexanol, (2) reduction, $NaBH_4$	Mt (Kunipia G, from Kunimine Co., Ltd.)	*E. coli*	CFU counting	Miyoshi et al. (2010)

(1) Stirring, $AgNO_3$ (60 °C, 8 h), (2) reduction: (a) $NaBH_4$, (b) UV-irradiation, (c) calcination	Mt (from Nanocor, USA) – unmodified (Nanocor PGN) – alkylammonium modified (Nanocor 1.44P)	*E. coli*, *S. aureus*, *K. pneumoniae*	CFU counting	Girase et al. (2011)
(1) Stirring, $AgNO_3$ (room temperature, 24 h), (2) reduction, $NaBH_4$	Mt (from Kunipa-F, Japan)	*E. coli*, *S. aureus*, *K. pneumoniae*	Disk diffusion method, inhibition zone determination	Shameli et al. (2011)
Shaking, $AgNO_3$ (room temperature, 24 h)	Mt (Ivančice, Czech Republic) – original and Na form of Mt	*E. faecalis*, *P. aeruginosa*	Broth dilution method, MIC determination	Hundáková et al. (2013a)
(1) Grinding, $AgNO_3$, with or without Na_2CO_3, (2) stirring in EG, → Ag, or Ag_2CO_3 NPs	Commercial Na-MT from Southern Clay Products (Gonzales, TX)	*E. coli*	Disk diffusion method, MIC determination	Sohrabnezdah et al. (2015)
(1) Stirring, $AgNO_3$, formaldehyde, NaOH, citric acid (3 h), (2) microwave-assisted method	Mt K-10 clay (from Sigma Aldrich)	*S. aureus*, *P. aeruginosa*	Disk diffusion and macrodilution methods	Kheiralla et al. (2014)
Adsorption, $AgNO_3$ (8 days)	Natural smectite (Mt) (North Patagonian, Argentina) – modified with silanizing agent APS or surfactant HDTMA	*E. coli*	Inhibition zone determination	Parolo et al. (2011)
Cation exchange, $AgNO_3$, used in package material	Mt – Na^+ form	Mesophilic, psychotrophic, and lactic acid bacteria, coliforms, yeasts, molds	CFU counting	Costa et al. (2011)
Cation exchange, $AgNO_3$, used in package material	Mt – Na^+ form	Mesophilic and psychotrophic bacteria, *Enterobacteriaceae spp.*, *Pseudomonas spp.*, yeasts, molds	CFU counting	Costa et al. (2012)
Shaking, $AgNO_3$ (room temperature, 24 h)	Ver (Santa Luzia, Brazil) – original and acidified by HCl	*P. aeruginosa*, *E. faecalis*	Broth dilution method, MIC determination	Hundáková et al. (2011)

(continued)

Table 14.1 (continued)

Method, precursor (conditions)	Inorganic substrate, chemical pretreatment	Tested bacteria	Testing method, test evaluation	Reference
Shaking, $AgNO_3$, $Cu(NO_3)_2$ (room temperature, 24 h)	Ver (Santa Luzia, Brazil)	*S. aureus*, *E. faecalis*, *K. pneumoniae*, *P. aeruginosa*	Broth dilution method, MIC determination	Hundáková et al. (2013b)
Shaking, $AgNO_3$, $Cu(NO_3)_2$ (room temperature, 24 h)	Ver (Santa Luzia, Brazil) Mt (Ivančice, Czech republic)	*E. coli*	Broth dilution method, MIC determination	Hundáková et al. (2014b)
Shaking (room temperature, 24 h), $AgNO_3$, $Cu(NO_3)_2$, used as filler into PE	Ver (Santa Luzia, Brazil)	*E. faecalis*	Broth dilution method, MIC determination, CFU counting	Hundáková et al. (2014a)
Adsorption, $AgNO_3$, $Cu(NO_3)_2$ (24 h)	Pal from the Mingguang palygorskite mine in Anhui Province of China – calcined and acid activated	*E. coli*, *S. aureus*	CFU counting	Zhao et al. (2006)
(1) stirring, $AgNO_3$ (room temperature, 24 h), (2) reduction, $NaBH_4$, shaking, $AgNO_3$ (room temperature, 24 h)	Talc (from Sigma Aldrich, St. Louis, MO)	*E. coli*, *S. aureus*	Disk diffusion method, inhibition zone determination	Shameli et al. (2011)
Cation exchange, $AgNO_3$, phosphoric acid	Kao, Sep, Cli (Eskisehir region) –Na^+ forms	*E. coli*	Halo test	Karel et al. (2015)
Shaking, $AgNO_3$ (24 h) – used as filler into PP	Kao (Sedlec, CZ) – (1) formamide, (2) NH_4Br, (3) vinylacetate + Bz_2H_2	*P. aeruginosa*, *E. faecalis*	Broth dilution method, MIC determination, CFU counting	Hundáková et al. (2016)
Shaking, $AgNO_3$ (24 h), reduction, $NaBH_4$	Hal (Henan province, China) – modification with silane coupling agent in toluene (refluxing 24 h)	*E. coli*, *S. aureus*	Inhibition zone determination, MIC determination, optical density	Zhang et al. (2013)
Adsorption, $AgNO_3$	Mexican zeolitic mineral clinoptilotite-heulandite (Taxco, Guerrero) – Na^+ form	*E. coli*, *S. faecalis*	CFU counting	Rivera-Garza et al. (2000)

Ag^+ bound electrostatically to Zeol	Zeol (Zeotomic AJ10N) (Sinanen Zeomic Co. Ltd., Nagoya, Japan)	*P. gingivalis*, *P. intermedia*, *A. actinomycetencomitans*, *S. mutans*, *S. sanguis*, *A. viscosus*, *S. aureus*	MIC determination	Kawahara et al. (2000)
Cation exchange, $AgNO_3$, $ZnNO_3{\cdot}5\ H_2O$, $Cu(NO_3){\cdot}2.5H_2O$ (shaking, 25 °C, 2 days)	Cli-rich Zeol mineral (Gördes, Turkey, Western Anatolia) – Na^+-rich form	*E. coli*, *P. aeruginosa*	Disk diffusion method	Top and Ülkü (2004)
Reflux, $AgNO_3$ (12 h) – use for disinfection of wastewater	Mexican zeol (Clinoptilotite-Heulandite) from Sonora	*E. coli*	CFU counting	Rosa-Gomez et al. (2008)
Reflux, $AgNO_3$ (12 h)	Mexican Cli (from Oaxaca and Sonora) – Na^+-rich form	*E. coli*	CFU counting	Rosa-Gomez et al. (2010)
Cation exchange, $AgNO_3$ (3× 24 h)	Cli (Marsid, Romania) – Na^+-rich form	*E. coli*, *S. aureus*	CFU counting	Copcia et al. (2011)
(1) Shaking, $AgNO_3$ (3 h), (2) reducing (550 or 700 °C, H_2 atm., 4 h)	Cli-rich tuff (Etla, Oaxaca, southeast Mexico) – Na^+-rich form	*E. coli*, *S. typhi*	CFU counting	Guerra et al. (2012)
Shaking, $AgNO_3$, $ZnNO_3{\cdot}5H_2O$, $Cu(NO_3){\cdot}2.5H_2O$, Benzalkonium chloride	Natural Zeol with 70wt.% Cli (the sedimentary deposit Zlatokop, Serbia Zeolite) – Na^+-rich form	*A. baumannii* – European clone I and II	CFU counting, MIC and MBC determination	Hrenovic et al. (2013)
Sol-gel dip coating – used to disinfection of wastewater	Natural Zeol (obtained from Afrand Tooska, Co. (Iran))	*Saprolegnia Sp.*		Johari et al. (2016)
Stirring, CTAB (room temperature, 16 h), $AgNO_3$	NaY Zeol (Zeolyst International, Havennummer, The Netherlands) –Na^+ rich	*E. coli*, *S. aureus*	MIC determination	Salim and Malek (2016)
Cation exchange, $AgNO_3$, $Cu(NO_3)_2$, $ZnCl_2$	Mt (Ivančice, Czech Republic), Ver (Letovice, Czech Republic)	*P. aeruginosa*, *E. faecalis*, *E. coli*, *T. vaginalis*	Broth dilution method, MIC determination	Pazdziora et al. (2010)

was investigated against *E. coli* (G^-), *Pycnoposus cinnabarinus* (*P. cinnabarinus*) and *Pleurotus ostreatus* (*P. ostreatus*), respectively. It was found that Ag-Mt composite was as effective as the free Ag^+ ions. Also, the inhibition of fungal growth on Ag-Mt composite was similarly active as free Ag^+ ions (Malachová et al. 2011).

Cation exchange method by dry way was used for incorporating of Ag^+ into bentonite (Ben) pre-treatment with HCl or H_2SO_4. Raw and acid activated Ben was subjected to an ion exchange process with melt of $AgNO_3$ and $NaNO_3$ at 435 °C. Authors studied antimicrobial properties of samples using bacteria *E. coli* (G^-) and *S. aureus* (G^+). Only Ben samples with Ag^+ showed antimicrobial effect. Moreover, the microbiological results showed influence of acid pre-treated of Ben on antimicrobial effect. Ben activated by HCl showed better bactericidal properties than Ben activated by H_2SO_4. The MIC value was for *S. aureus* 0.022 g of sample Ag^+-HCl-Ben and 0.038 g of Ag^+-H_2SO_4-Ben and for *E. coli* 0.012 g of sample Ag^+-HCl-Ben and 0.038 g of Ag^+-H_2SO_4-Ben (Santos et al. 2011).

Xu et al. (2011) introduced a novel way of preparation of Ag-Mt material with antibacterial activity exhibiting slow release property. At first, transparent $[Ag(NH_3)_2]$ OH aqueous solution was prepared by adding $NH_3.H_2O$ to Ag_2O powder. The solution was mixed with Mt and stirred at 60 °C in the dark. Mixture was added to poly (N-vinyl-2-pyrrolidone (PVP) and UV-irradiated at room temperature. Results shown, that after UV irradiation the Ag^+ turned into metallic Ag^0 NPs. This indirectly suggested change of Ag-Mt color from milk-white to black after irradiation. Antibacterial activity was tested against *E. coli* (G^-). The MIC value was 100×10^{-6} of Ag-Mt and the sterilizing efficiency (SE) was reaching 100%. Even after five times washes with distilled water, the MIC value of sample was 200×10^{-6} and the SE was more than 99%. Authors confirm slow release property of Ag from Mt substrate which can be explain by strong interactional force between Ag NPs and Mt due to a large Mt surface area and small diameter of Ag NPs (Xu et al. 2011). Antibacterial activity of Ag-Mt prepared using original Mt and Na^+-form of Mt was compared. The monoionic Na^+-form of Mt (Na^+Mt) was prepared using the most common cation exchanged process with NaCl aqueous solution. Original Mt and Na^+Mt were shook with $AgNO_3$ aqueous solution (protected by aluminum foil against the light). Total amount of Ag determined in samples was from 0.64 to 4.47 wt.% depending on initial concentration of $AgNO_3$ solution and used matrix (Mt or Na^+Mt). Samples prepared from monoionic Na^+Mt form contained higher amount of Ag and showed better inhibition effect on both tested bacteria *P. aeruginosa* (G^-) and *E. faecalis* (G^+) (Hundáková et al. 2013a).

The interesting studies were focused to application of Ag-Mt to packaging materials (Costa et al. 2011, 2012). In one study, prepared Ag-Mt samples were used to improve the shelf life of fresh fruit salad. The sensorial and microbiological quantity was determined. The microbiological activity was evaluated by monitoring the principal spoilage microorganisms (mesophilic and psychotropic bacteria, coliforms, lactic acid bacteria, yeasts and molds). Results show that a significant shelf life prolongation of fresh fruit salad can be obtained by a straightforward new packaging system by using Ag-Mt (Costa et al. 2011). In second study, the effect of active coating loaded with Ag-Mt and film barrier properties on shelf life of fresh

cut carrots were investigated. The sensorial and microbiological quality was observed. For microbiological quality, the spoilage microorganisms as mesophilic and psychotropic bacteria, *Enterobacteriaceae* spp., *Pseudomonas* spp., yeasts and moulds were used. For sensorial evaluation, color, odor, firmness and product overall quality were evaluated) (Costa et al. 2012). Cao et al. (2014) published very interesting study about sutures modified by Ag^+ loaded Mt (Ag^+ Mt/sutures). The antibacterial properties of prepared materials were tested using bacteria *E. coli* (G^-) and *S. aureus* (G^+). Moreover, hemolysis tests and in vitro cytotoxicity test of Ag^+ Mt/sutures were determined. The Ag^+ Mt/sutures exhibited good blood and tissue biocompatibilities. In addition, the Ag^+ Mt/sutures inhibited growth of *E. coli* by 99% (Cao et al. 2014).

Several authors published study about antibacterial activity of Ag NPs prepared on substrates by the chemical reduction method with borohydride ($NaBH_4$) as reducing agent.

Mt was shaken with $AgNO_3$ aqueous solution at room temperature. To dried sample the $NaBH_4$ aqueous solution was added and reduction under shaking took for several minutes. Antibacterial activity of Ag^+ ions and metallic Ag^0 prepared on Mt substrate was tested on *E. coli* (G^-) and *E. faecium* (G^+). The metallic Ag^0 showed no antibacterial effect (Malachová et al. 2009). The Ag NPson the surface and in the interlayer space of Mt was prepared by $NaBH_4$ reduction in n-hexanol. Antibacterial activity against *E. coli* (G^-) was determined by counting the CFU (colony forming unit) number. Samples were tested in the dark and under room light when a stronger antibacterial effect was observed. Authors also tested and confirmed antibacterial activity of samples after 12 years what confirmed their stability and suitability for application to industry use (Miyoshi et al. 2010). Shameli et al. (2011) synthesized Ag NPs on Mt with the mean diameter of Ag NPs from 4.19 to 8.53 nm. The particles size increased with increased concentration of initial Ag^+ ions. Moreover, intercalated structure of Mt was confirmed in Ag-Mt nanocomposites. Antibacterial activity was tested for $AgNO_3$-Mt suspension and Ag-Mt nanocomposites on the G^- bacteria *E. coli* and *K. pneumoniae* and the G^+ bacteria *S. aureus*. Results showed that measured inhibition zone for $AgNO_3$-Mt and Ag-Mt nanocomposites were similar for both type of bacteria. The antibacterial activity of Ag-Mt nanocomposites decreased with increased of Ag NPs particles size (Shameli et al. 2011). Girase et al. (2011) prepared Ag on Mt substrate, which was used as untreated or organically modified and both ball milling, by three methods (Fig. 14.1). The Ag NPs size on Mt depended on used method. The size distribution of the Ag NPs on Mt followed the sequence: UV > Calcined > $NaBH_4$ reduced. The Ag NPs synthesized in the absence of Mt by all three method (calcination, $NaBH_4$ reduction and UV irradiation) were larger (~60–200 nm) than the particles precipitated on Mt (5–25 nm). Results confirmed that the shape and size of NPs can depend on used substrate, preparation conditions and used method. Difference in size of Ag NPs synthetized on Mt substrate by three various methods is show in Fig. 14.1. Moreover, the Ag NPs precipitated ex-situ in solution prepared to compare. The both ex situ Ag NPs and in situ precipitated Ag NPs on Mt indicated antibacterial activity against *E. coli* (G^-) as a function of time. In situ precipitated

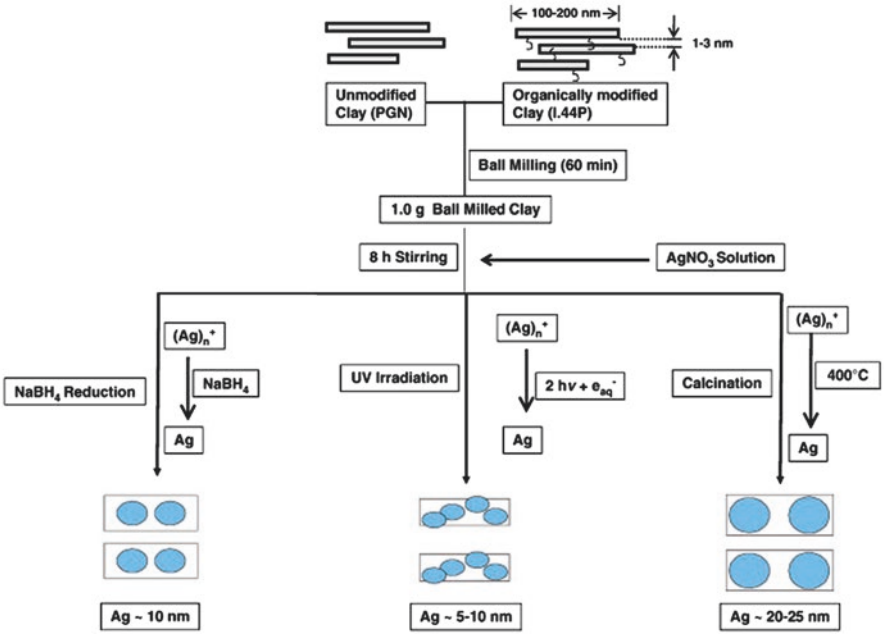

Fig. 14.1 Schematic illustration of the synthesize Ag NPs-Mt nanohybrid material (*in-situ* precipitation of Ag NPs on the Mt surface). Reproduced with permission from (Girase et al. 2011), © 2011, Elsevier B.V

Ag NPs on Mt indicated good antibacterial performance, irrespective of the method used to Ag preparation (reduction, calcination or UV method). In the case of Ag NPs-Mt nanohybrid structure, the CFU number of *E. coli* decreased by four orders of magnitude as compared to samples without Ag. Authors observed that the behavior of antimicrobial activity is related to the behavior of release of Ag ions from Mt (Fig. 14.2) (Girase et al. 2011).

Sohrabnezdah et al. (2015) used Na^+Mt as stabilizer for preparation of Ag_2CO_3 and Ag NPs in aqueous and polyol solvent. Different treatments were used: In first, Mt with $AgNO_3$ and Na_2CO_3 were ground and ethylene glycol (EG) was added under stirring. In second, the same procedure was used without Na_2CO_3. The metallic Ag^0 in these Mt nanocomposites was confirmed. In third, the same method was used with water instead EG. This process led primarily to the formation of Ag_2CO_3 NPs in nanocomposite. Moreover, results also show Ag^0 NPs present and probable the intercalation of both Ag and Ag_2CO_3 NPs into the Mt gallery. Results of antibacterial test on *E. coli* (G^-) showed that the Ag_2CO_3-Mt nanocomposite exhibited an antibacterial activity higher than Ag-Mt. Authors explained higher antibacterial action of the Ag_2CO_3-Mt by higher release of Ag^+ ions from Ag_2CO_3 and interaction with bacterial strain. In case of Ag NPs on Mt surface, less Ag^+ ions are oxidatively released from Ag NPs surface.

Kheiralla et al. (2014) synthetized the Ag NPs on Mt substrate using the microwave assisted method. The Ag NPs-Mt nanocomposites were prepared by mixing of

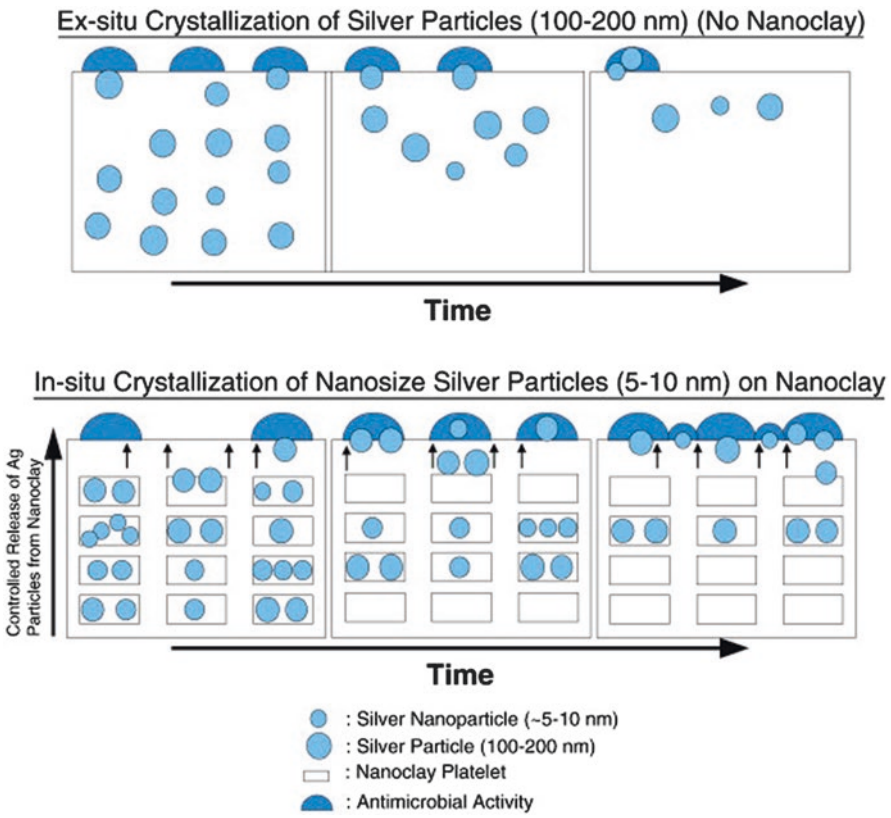

Fig. 14.2 Schematic illustration of diffusion-controlled release of Ag ions from clay platelets (in-situ precipitated Ag NPs) and ex-situ precipitated Ag NPs in solution and their antimicrobial behavior. Reproduced with permission from (Girase et al. 2011), © 2011, Elsevier B.V

aqueous solution $AgNO_3$ with Mt. Formaldehyde and NaOH aqueous solution was added until the pH was 10 and citric acid was added. The solution was placed in a microwave. The samples with the weight ratio 1, 3 and 5% of Ag in Mt were prepared. The diameter of synthetized Ag NPs on Mt was below 15 nm. Antibacterial activity was evaluated against bacteria *S. aureus* (G^+) and *P. aeruginosa* (G^-). The maximum inhibition zone diameters for concentration of Ag 1, 3 and 5% were determined for *S. aureus* as 29, 39 and 45 mm and for *P. aeruginosa* as 10, 25 and 37 mm, respectively. The MIC value of Ag NPs was determined as 0.031 mg for both bacteria, while the MBC value was 0.5 mg for *S. aureus* and 0.25 mg for *P. aeruginosa*. Moreover, the synergistic effect of Ag NPs and antibiotics was observed.

Vermiculite (Ver) is used as substrate for Ag NPs preparation very sporadically.

The Ag NPs were prepared on Ver matrix by shaken of Ver with $AgNO_3$ aqueous solution at room temp. The size of Ag NPs on Ver surface was heterogeneous, from smaller than 20–50 nm. Antibacterial action of samples started after 1–1.5 h against G^- bacteria *S. aureus* and *E. faecalis* and after 2–3 h against G^+ bacteria *K. pneu-*

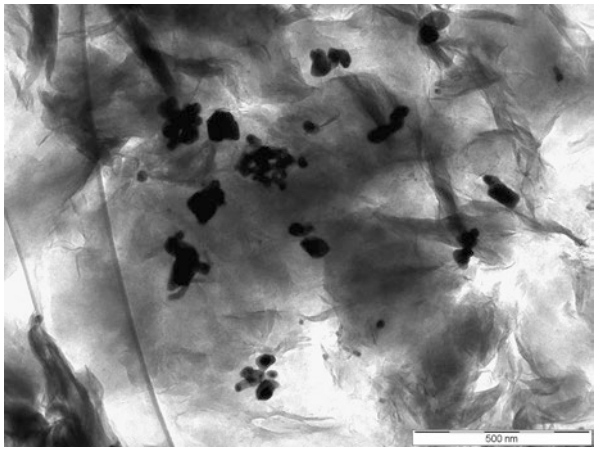

Fig. 14.3 TEM images of Ag NPs on Mt substrate

moniae and *P. aeruginosa* and action was persisting for the whole testing period 6 days. Moreover, authors studied release of Ag^+ from Ver matrix into the water environment, which was determined as 0.1–0.4% from the total Ag content in samples. The Ag NPs on Mt were prepared by the same method. The amount of silver in Ag-Ver was higher than in Ag-Mt samples. The Ag NPs grew with a similar size on Mt and Ag NPs size was heterogeneous on Ver. The antibacterial action of Ag-Ver samples was better than Ag-Mt samples (Valášková et al. 2010). The original and acidified Ver (with HCl) were compared as substrates for precipitation and growth of Ag NPs. The MIC values of samples against bacteria *P. aeruginosa* (G^-) and *E. faecalis* (G^+) were from 10% (w/v) to 0.37% (w/v) (Hundáková et al. 2011). The antibacterial activity of Ag-Ver, Cu-Ver and Ag, Cu-Ver materials was investigated. The inhibition effect on bacterial growth was confirmed in all prepared Ag-, Cu-Ver samples. The synergic effect of Ag and Cu in combined samples was observed (Hundáková et al. 2013b). The antibacterial properties of Ag and Cu prepared on two clay mineral matrices Mt and Ver were compared. The transmission electron microscopy (TEM) images of the Ag NPs reduced on Mt and Ver substrate are show in Figs. 14.3 and 14.4. Results of antibacterial test on *E. coli* (G^-) show good inhibition effect on bacterial growth. Moreover, stability of Ag^+ and Cu^{2+} on both matrices in water environment was studied and the relationship between amount of metal ions released from samples and antibacterial effect was confirmed (Hundáková et al. 2014a). The Ag-Ver, Cu-Ver and Ag-Cu-Ver were used as nanofillers to polyethylene (PE) matrix for a purpose to obtain the antibacterial PE material. Antibacterial properties of powder Ver nanofillers and surfaces of PE/Ver composites was tested on the G^+ bacteria *E. faecalis*. Samples Ag-Ver and AgCu-Ver showed the MIC value 10% (w/v) after 1 h and 3.33% (w/v) after 24 h. The sample Cu-Ver was slightly less effective and showed MIC value 10% (w/v) after 5 h and 3.33% (w/v) after 48 h of inhibition. The surfaces of all tested PE/Ver-Ag,Cu composites showed inhibition effect after 24 h in comparison to pure PE. The CFU number decreased from the countless number to several hundred colonies (Hundáková et al. 2014b).

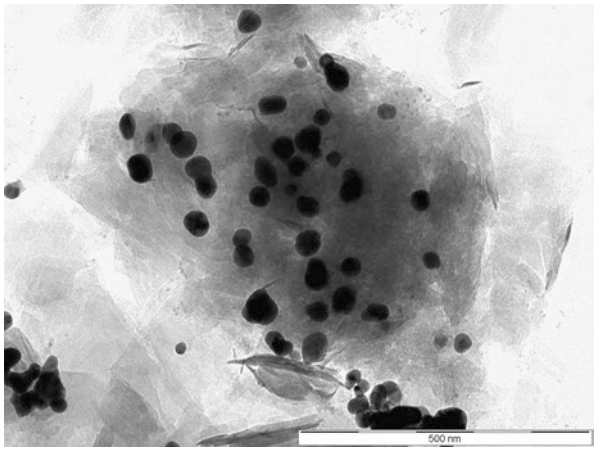

Fig. 14.4 TEM images of Ag NPs on Ver substrate

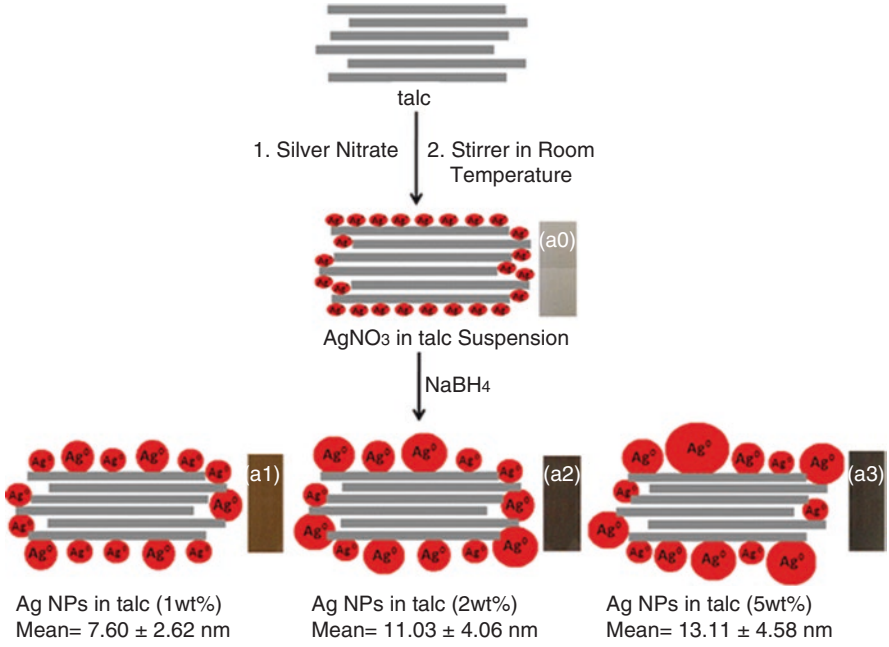

Fig. 14.5 Schematic illustration of the synthesis of Ag NPs-talc composite material by the chemical reduction. The color change of AgNO3/talc suspension during process was from colorless (a0) to light brown (a1), brown (a2) and dark brown (a3) according the Ag NPs content. Reproduced with permission from (Shameli et al. 2013), © Springer Science+Business Media Dordrecht 2013

Clay minerals as talc, palygorskite, kaolinite, halloysite, sepiolite, etc. are very rarely used for metal nanoparticles preparation for a purpose to study their antibacterial activity.

Nevertheless, the Ag NPs were synthetized on the talc surface by the wet chemical reducing method with the $NaBH_4$ solution (Fig. 14.5). The mean diameter of Ag

NPs anchored on talc surface was from 7.60 to 13.11 nm. Antibacterial activity of prepared samples was tested on bacteria *E. coli* (G^-) and *S. aureus* (G^+). Ag NPs-talc nanocomposite did not show any inhibition effect in contrast with $AgNO_3$ -talc which inhibited the bacterial growth. Authors studied also Ag^+ release from talc structure, which was fast at the beginning of experiment and becomes slower in time. The Ag^+ release from Ag NPs-talc nanocomposites can last for more than 16 days (Shameli et al. 2013).

The Ag- or Cu-Pal were prepared for purpose to removing bacteria from aqueous solution. Antibacterial testing was performed using *E. coli* (G^-) and *S. aureus* (G^+) as indicators of fecal contamination of water. The Ag- and Cu-Pal eliminated the pathogenic organisms from water after 12 h of contact time. Antibacterial test showed no activity of untreated Pal. The CFU number of *E. coli* decreased from initial 1.6×10^4 CFU to 0 CFU after 6 h in contact with Ag-Pal (0.6% Ag). For the same sample, the CFU number of *S. aureus* decreased from initial 1.5×10^4 CFU to 0 CFU after 12 h in contact. The CFU number of *E. coli* decreased to 0 CFU after 12 h and the CFU number of *S. aureus* decreased to 0 CFU after 24 h in contact with Ag-Pal (0.57% Cu). Authors showed the differences in the results to the structural differences in bacteria cell walls, concretely to a thicker cellular wall of *S. aureus.* The results of water erosion test indicated that Ag and Cu amount remained on 80.2% and 72.5% in samples after 72 h in contact with water, respectively (Zhao et al. 2006).

Zhang et al. (2013) used Hal nanotubes as a support of Ag NPs. Hal was modified with [3-(2-aminoethyl) aminopropyl] trimethoxysilane in toluene. Modified Hal was mixed with $AgNO_3$ methanol solution and reduction of Ag NPs with $NaBH_4$ aqueous solution was performed. The Ag NPs (average diameter about 5 nm) were uniformly distributed across the surface of Hal. Results of antibacterial test show the diameter of inhibition zone 12 mm for *E. coli* and 13 mm for *S. aureus*. The photographs of samples solutions in agar plates after 16 h exposure to bacteria *E. coli*, compared with the control, shows that Ag NPs and Ag NPs-Hal reaches antibacterial rate of 94.58% and 100%, respectively. Authors ascribed the higher antibacterial activity of Ag-NPs-Hal to the large surface area of the Ag-NPs on Hal. The Ag-NPs in suspension could aggregate what leads to reduce their effective surface area and worse inhibition activity. The quantitative antibacterial properties showed the MIC value 64 μg/mL of Ag-NPs and 32 μg/mL of Ag-NPs-Hal.

Karel et al. (2015) prepared antibacterial Ag-Kao, Ag-Clinoptilotite (Cli) and Ag-Sep. Samples with Ag were prepared by ion exchange of Na^+-forms of Kao, Cli and Sep with $AgNO_3$ aqueous solution during continuously stirring at a dark environment (physical treatments). Prepared materials were subjected to phosphoric acid solution (chemical treatments). The amount of silver incorporated in samples was by chemical treatment: 0.13 wt.% in Kao, 0.65 wt.% in Cli, and 0.75 wt.% in Sep and by physical treatment: 0.84 wt.% in Kao, 0.70 wt.% in Cli, and 0.79 wt.% in Sep. Chemically treated clays contained about 1.5 wt.% of Phosphorous. In samples treatment with phosphoric acid, the amount of Ag in samples was higher. Antibacterial halo test (Fig. 14.6) against *E. coli* (G^-) showed that the physically treated clays exhibited greater circular zone diameter (25–28 mm) in comparison with chemically

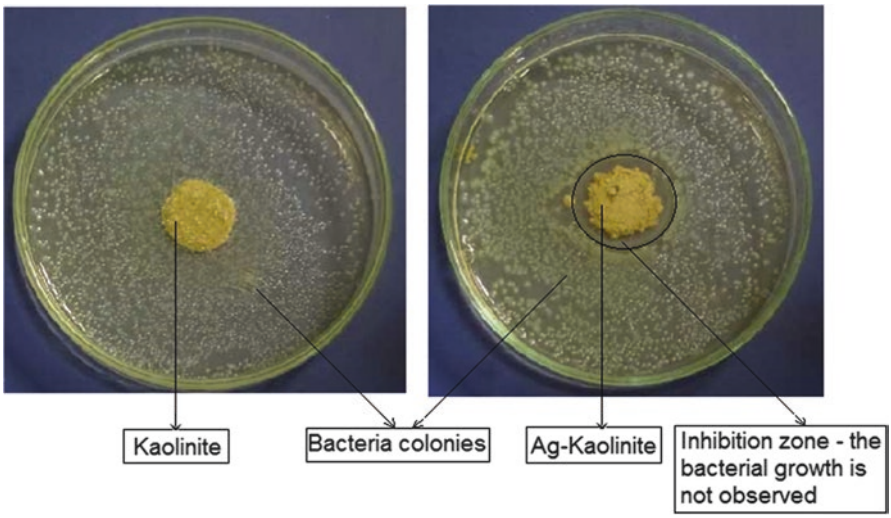

Fig. 14.6 Illustration of inhibition zone determination from antibacterial (modified halo) test. Adapted from (Karel et al. 2015)

treated clays (22–24 nm). Results of Ag release showed that Ag in chemically treated samples is more stable opposite physically treated samples. The amount of residual Ag in samples after 30 days of exposure to water was for chemical treatment samples: 0.06 wt.% in Kao, 0.26 wt.% in Cli, and 0.19 wt.% in Sep and for physical treatment samples: 0.70 wt.% in Kao, 0.54 wt.% in Cli, and 0.36 wt.% in Sep.

Antibacterial Ag-Kao samples were prepared by chemical modification of Kao pre-treatment with formamide, ammonium bromide, benzoylperoxide and vinylacetate monomer (polymerization in-situ) and subsequent treatment with $AgNO_3$ aqueous solution. Prepared materials were used as nanofillers to polypropylene (PP) matrix and antibacterial properties of PP/Ag-Kao composites were studied on the bacteria *E. faecalis* (G^+) and *P. aeruginosa* (G^-). Results show that inhibition effect increased with increasing content of Ag-Kao nanofiller in PP/Ag-Kao composite. Nevertheless, tested *E. faecalis* exhibited higher sensitivity to action of PP/Ag-Kao composites than *P. aeruginosa* and the CFU number of *E. faecalis* decreased about 100% after 24 h of contact time with surface of PP/Ag-Kao composite (Hundáková et al. 2016).

Antibacterial zeolite material as a new antibacterial agent was described already in 1987 (Maeda 1987). Zeol are widely used as adsorbents in wastewater treatment, so their using as water filter media is possible. For example, water adsorption properties of Ag- and Zn-exchange Zeol were studied (Benaliouche et al. 2015).

The antibacterial effect of Zeol exchanged with Ag was tested on *E. coli* (G^-) and *S. aureus* (G^+) by number viable bacterial colonies (NVC) counted. Zeo was pretreated to Na^+Zeo and put into contact with $AgNO_3$ solutions (Ag-Zeo). Antibacterial effect is dependent on Ag content in Ag-Zeo samples. Nevertheless, the NVC of *E. coli* decreased to 0 after 2 h and the NVC of *S. faecalis* decrease to

0 after 6 h in contact with the same samples. The Na^+Zeo mineral without Ag not showed antibacterial behavior (Rivera-Garza et al. 2000). Antibacterial effect of Ag-Zeol on oral bacteria under anaerobic conditions was studied. The oral bacteria *Porphyromonas gingivalis* (*P. gimgivalis*), *Prevotella intermedia* (*P. intermedia*), *Actinobacillus actinomycetencomitans* (*A. actinomycetencomitans*), *Streptococcus mutans* (*S. mutans*), *Streptococcus sanguis* (*S. sanguis*), *A. viscosus* and *S. aureus* were used. The MIC values were between 256 and 2,048 μg/ml of Ag-Zeol which corresponded to 4.8–38.4 μg/ml of Ag^+. Release of Ag^+ into the broth was also measured. Results of antibacterial test show that bacteria *P. gingivalis*, *P. intermedia*, *A. actinomycetencomitans* were more sensitive to the action of Ag-Zeol samples. According the study, Ag-Zeol may be a useful to provide antibacterial function for dentistry materials (Kawahara et al. 2000).

The water disinfecting behavior of Ag-modified Zeol was investigated (Rosa-Gomez de la et al. 2008, 2010). The ion exchange reaction was involved: Na^+Zeol + $AgNO_3 \leftrightarrow$ Ag-Zeol + $NaNO_3$. The water disinfecting behavior of Ag-modified Zeol was studied using *E. coli* (G^-) bacteria as indicator of microbiological contamination of water in a column system. Glass columns were filled with tested samples and loaded with synthetic wastewater with *E. coli* or municipal wastewater polluted with coliform microorganisms. In both wastewaters the initial microorganism concentration was around 10^7 NVC/100 ml. The wastewater was pumped through the column at a flow rate of 2 ml/min. The Ag concentration and microorganisms were monitored. The average amount of Ag^+ in Ag-Zeol was 4.33 wt.% (0.4009 meq Ag/g). After complete disinfection processes, it was found that 16.6% and 0.6% of *E. coli* survival. The amounts of silver determined in effluents were 220.9 and 305.7 μg corresponding to 5.1% and 3.5% of the initial Ag. When the silver effluent was less than 0.6 μg/ml, the *E. coli* percentage increased and the volume of disinfected water diminished. After complete disinfection processes, 100% of coliform microorganism's survival was recorded. The amount of silver determined in effluents were 263.7 and 222.4 μg corresponding to 6.1% and 2.5% of the initial Ag. The Na-Zeol sample did not show antibacterial activity in both cases. Moreover, authors studied interference of NH^{4+} and Cl^- ions on the disinfection process. They found that the presence of NH^{4+} ions improves the antibacterial activity of Ag-Zeol on *E. coli* and the presence of Cl^- ions notably diminished the antibacterial activity (Rosa-Gomez de la et al. 2008).

Natural Cli-rich tuff was first pre-treated with oxalic acid (followed by treatment with NaCl solution) (P1) and NaOH solution (P2). Samples were cation exchanged with $AgNO_3$ aqueous solution. The amount of Ag in samples was 1.9 meq Ag/g in the P1-Ag^+ and 1.2 meq Ag/g in the P2-Ag^+. The antibacterial effect of P1-Ag^+ sample was observed stronger for the growth of *E. coli* (G^-) (18% CFU/ml) opposite *S. aureus* (G^+) (31.58% CFU/ml). Conversely, the antibacterial effect of P2-Ag^+ sample was observed stronger for the growth of *S. aureus* (62.71% CFU/ml) opposite *E. coli* (74% CFU/ml). The antibacterial action of sample prepared from Cli pre-treated with oxalic acid and NaOH was more effective in comparison with sample pre-treated with NaOH due to the different content of Ag (Copcia et al. 2011).

Guerra et al. (2012) evaluated Ag-Cli as a biocide for the G^- bacteria *E. coli* and *S. typhi*. The Ag-Cli samples were prepared by shaking of Na^+Cli with $AgNO_3$ solu-

tion and by reduction at 550 or 700 °C under H_2. The Ag content in samples was determined as 2.1 wt.% and 4.0 wt.%. The X-ray diffraction patterns of samples with higher amount of Ag show well-defined narrow peaks of metallic Ag NPs. The size distribution of Ag NPs (spherical shape) determined was in the range 0.7–9.2 nm depending on the amount of Ag in samples and on reducing temperature. Study of biocidal effect on *E. coli* show that Ag-Cli samples (0.06 g per 18 ml of culture media) with 4 wt.% or 2 wt.% of Ag eliminated all colonies during 30 min and 120 min, respectively. The higher amount of samples was needed to achieve similar inhibition for *S. typhi*. The Ag-Cli samples (0.12 g per 18 ml of culture media) with both 4 wt.% or 2 wt.% of Ag eliminated all colonies during 5 min. It was concluded that the shape and size of the Ag NPs dispersed on the support are not crucial for biocidal effect at high concentration of Ag. Authors also found that Ag did not leach from samples during the experiment with both bacteria, thus the biocidal material can be reused.

Hrenovic et al. (2013) prepared Ag-Zeol, Cu-Zeol and benzalkonium (BC)-Zeol materials and confirmed their antibacterial activity against isolates of *A. baumannii* (Eropean clone I (EUI) and II (EUII). Samples Ag-Zeol, Cu-Zeol and BC-Zeol contained 50.65 mg Ag^+, 20.33 mg Cu^{2+} and 85.0 mg BC per gram, respectively. The *A. baumannii* from EUII was more sensitive to Ag-Zeol and Cu-Zeol with the MBC value 31.2 mg/l and 125 mg/l, respectively opposite EUI with MBC value 250 mg/l for both samples. Authors compared antibacterial activity of Ag, Cu, BC-Zeol samples with Ag, Cu, BC cations. Results show that the modified Zeol did not show the pronounced activity opposite Ag, Cu and BC salts. The main reason is their stability and slow release of cations from modified Zeol.

The starting material NaY-Zeol was pre-treated with cetyltrimethyl ammonium bromide (CTAB). The CTAB-modified NaY Zeol was regenerated to NaY Zeol using thermal treatment calcination at 550 °C. The regenerated NaY Zeol was cation exchange to Na-form because Na^+ in Zeol could be easily exchange with Ag^+. The AgY Zeol samples with different Ag amount were prepared by mixing of regenerated NaY Zeol with $AgNO_3$ aqueous solution. The amount of silver in AgY samples was 9 mg/g, 63 mg/g and 90 mg/g with increasing concentration of initial $AgNO_3$ solution. Results of antibacterial testing show that AgY Zeol sample had better inhibition effect on *E. coli* in comparison with *S. aureus* in distilled water, while both bacteria showed low sensitivity to samples in saline solution. The MIC value decreased with increasing content of Ag in samples (Salim and Malek 2016). The next interesting study was published about studied of Ag NPs-coated Zeol as water filter media for fungal disinfection of rainbow trout eggs (Johari et al. 2016).

14.2.2 Copper on Clay Minerals

Copper can be prepared on inorganic substrates by several methods as Cu^{2+} cations or Cu, CuO and Cu_2O nanoparticles. The most frequently used method of Cu^{2+} is preparation by cation exchange on clay substrates, while the most widely used is

montmorillonite. Summary of some preparation methods of copper on the various substrates, bacterial strains and testing methods used for studying the antimicrobial activity is shown in Table 14.2.

The antibacterial ability of Cu^{2+}-Mt was studied on *E. coli* (G^-) and *S. aureus* (G^+) bacteria. The MIC value of Cu^{2+}-Mt on these bacteria was 10 mg/l (equal to amount of Cu^{2+} ~ 100 ppm) after 24 h and 50 mg/l (equal to Cu^{2+} ~ 500 ppm) after 6 h and 4 h, respectively. The MIC value of Cu^{2+}- Mt for both bacteria was 200 mg/l after 2 h of action. The Cu^{2+} concentration released from Mt was determined after 2 h of incubation as 0.07 mg/l from 10 mg/l Cu^{2+}-Mt and 1.61 mg/l from 200 mg/l Cu^{2+}-Mt (Zhou et al. 2004). The antibacterial activity of Cu^{2+}-Mt was tested against the G^- bacteria *Aeromonas hydrophila* (*A. hydrophila*). The MIC and minimum bactericidal concentration (MBC) of Cu^{2+}-Mt were found to be 150 and 600 mg/l, respectively (Hu et al. 2005). The other authors published study about antibacterial effect of Cu^{2+}-Mt on two G^- bacterial strains *E. coli* and *Salmonella choleraesius* (*S. choleraesius*) and the MIC value of Cu^{2+}-Mt was found as 1,024 μg/ml and 2,048 μg/ml, respectively. Authors divided the antibacterial process to two stages: adsorption of bacteria from solution and immobilization on the Cu^{2+}-Mt surface and action related to accumulation of Cu^{2+} on the Mt surface. The release concentration of Cu^{2+} ions from Mt into the broth increased with their increasing amount in Cu^{2+}-Mt. Nevertheless, the released amount of Cu^{2+} from Cu^{2+}-Mt into the broth was very low. The effect of Cu^{2+}-Mt on bacterial cell walls, on enzyme activity of bacteria and on the respiratory metabolism of bacteria was confirmed (Tong et al. 2005). The original CaMt, monoionic form NaMt and acid activated (AA)Mt were cation exchange with $CuSO_4$ to Cu^{2+}-CaMt, Cu^{2+}-NaMt and Cu^{2+}-AAMt. The antibacterial activity was tested on *E. coli* (G^-). The initial CaMt, NaMt and AAMt showed reducing of bacterial plate counts by 14.2%, 13.4% and 37.4%, respectively. Nevertheless, the Cu^{2+}-CaMt, Cu^{2+}-NaMt and Cu^{2+}-AAMt showed reducing of bacterial plate counts by 95.6%, 97.5% and 98.6%, respectively (Hu and Xia 2006).

In order to use in veterinary medicine, the Cu^{2+}-Mt was also studied in relating to the effect on the growth performance and intestinal microflora of weanling pigs. The weanling pigs (total 128 pigs with initial average weight 7.5 kg) were divided into four groups according the dietary treatments in single doses adjusted follows: (1) basal diet, (2) basal diet +1.5 g/kg Mt, (3) basal diet +36.75 mg/kg $CuSO_4$ (with the Cu^{2+} equivalent to that in Cu^{2+}-Mt) and (4) basal diet +1.5 g/kg Cu^{2+}-Mt. Experiment was carried out for 45 days. Effect of diet was studied on intestinal microflora (total aerobes, total anaerobes, *Bifidobacterium*, *Lactobacillus*, *Clostridium*, *E. coli*) in both small intestine and proximal colon of pigs. The diet supplemented with Mt and $CuSO_4$ had no effect on growth performance, intestinal microflora and enzyme activities. Pigs fed with Cu^{2+}-Mt had reduced total viable counts of *Clostridium* and *E. coli* in the small intestine and proximal colon opposite control. The improvement of growth performance of weanling pigs and reduced of bacterial enzyme activities were found (Xia et al. 2005). The effect of two Cu^{2+} exchanged Mt, concrete Cu^{2+}-CaMT and Cu^{2+}-NaMt were studied as alternative agents to chlortetracycline. The growth performance, diarrhea, intesti-

Table 14.2 Summary of methods and precursors used for the preparation of copper on the inorganic substrates, used testing methods, and bacterial strains for studying the antimicrobial activity of prepared materials

Method (conditions), precursor	Inorganic substrate, chemical pretreatment	Tested bacteria	Testing method/test evaluation	Reference
Cation exchange (stirring, 60 °C, 6 h), $CuSO_4 \cdot 5H_2O$	Mt (Chifeng, the Inner Mongolia Autonomous Region, China)	*E. coli, S. faecalis*	MIC determination	Zhou et al. (2004)
Cation exchange (stirring, 60 °C, 6 h, pH 5), $CuSO_4 \cdot 5H_2O$	Mt (Inner Mongolia Autonomous Region, China) – pretreated to Na^+ form	*A. hydrophila*	MIC and MBC determination – broth dilution method	Hu et al. (2005)
Cation exchange (agitating 24 h), $CuSO_4 \cdot 5H_2O$	Mt (Inner Mongolia Autonomous Region, China)	*E. coli*, *S. choleraesuis*	MIC determination	Tong et al. (2005)
Cation exchange (stirring, 60 °C, 6 h, pH 5), $CuSO_4 \cdot 5H_2O$	Ca-Mt (Inner Mongolia Autonomous Region, China) – Na^+ form and acid activated Mt	*E. coli*	CFU counting	Hu and Xia (2006)
Cation exchange (stirring, 60 °C, 6 h, pH 5), $CuSO_4 \cdot 5H_2O$	Mt (Inner Mongolia Autonomous Region, China)	Intestinal microflora of pigs	CFU counting	Xia et al. (2005)
Cation exchange (stirring, 60 °C, 6 h, pH 5), $CuSO_4 \cdot 5H_2O$	Mt (Inner Mongolia Autonomous Region, China), Mt pretreated to Na^+ form	Intestinal microflora of pigs		Song et al. (2013)
Cation exchange (stirring, 60 °C, 6 h, pH 5), $CuSO_4 \cdot 5H_2O$	Mt (Inner Mongolia Autonomous Region, China), Mt pretreated to Na^+ form	Intestinal microflora of Nile tilapia	CFU counting	Hu et al. (2007)
Shaking (24 h, room temperature), $AgNO_3$, $Cu(NO_3)_2$, $Zn(NO_3)_2$, CP	Mt (Middle Anatolia) – purified	*S. aureus*, *P. aeruginosa*	Disk diffusion method	Özdemir et al. (2010)
Shaking (24 h, room temp.), $AgNO_3$, $ZnSO_4$, $CuSO_4$	Na^+-rich Mt (SWy2) (Crook County, Wyoming)	*E. coli*, *P. cinnabarinus*, *P. ostreatus*	CFU counting, median effective concentration (EC50)	Malachová et al. (2011)

(continued)

Table 14.2 (continued)

Method (conditions), precursor	Inorganic substrate, chemical pretreatment	Tested bacteria	Testing method/test evaluation	Reference
In situ reduction of a copper ammonium complex, → Cu NPs $CuCl_2{\cdot}2H_2O$, hydrazine	Mt (Nanocor Inc., SA) – pretreated to Na^+ form	*E. coli*, *S. aureus*, *P. aeruginosa*, *E. faecalis*	CFU counting, MBC calculation, cytotoxicity test	Bagchi et al. (2013)
Thermal decomposition method, → CuO NPs (600°C) $CuSO_4{\cdot}5H_2O$, Na_2CO_3	Commercial Na-MT purcheased. from Southern Clay Products (Gonzales, TX)	*E. coli*	MIC determination, disk diffusion method	Sohrabnezdah et al. (2014)
Cation exchange (stirring, 80 °C, 3 h), $CuCl_2{\cdot}2H_2O$ (Cu-Ver heated at 200 or 400 °C, 3 h)	Ver (Yli County in Xinjiang, China)	*E. coli*	Halo method	Li et al. (2002)
Cation exchange (80 °C, 3 × 2 h) $CuCl_2$, $AgNO_3$, $ZnCl_2$	Mt (Ivančice, Czech Republic), Ver (Letovice, Czech Republic)	*E. faecalis, E. coli*, *P. aeruginosa*, *T. vaginalis*	MIC determination	Pazdziora et al. (2010)
Cation exchange (stirring, 70–80 °C, 4–12h), $CuSO_4{\cdot}5H_2O$ H_2 reduction (Ar flow to 400–600°C, H_2 or air flow 2–3h) → Cu NPs	Two commercial exfoliated Ver from Virginia Vermiculite LLC – Grade No. 5 and Milled No. 7	*S. aureus*	Disk diffusion test	Drelich et al. (2011)
Shaking (24 h, room temperature), $AgNO_3$, $Cu(NO_3)_2$	Ver (Santa Luzia, Brazil)	*S. aureus*, *E. faecalis*, *K. pneumoniae*, *P. aeruginosa*	Broth dilution method, MIC determination	Hundáková et al. (2013b)
Shaking (24 h, room temperature), $AgNO_3$, $Cu(NO_3)_2$	Ver (Santa Luzia, Brazil) Mt (Ivančice, Czech Republic)	*E. coli*	Broth dilution method, MIC determination	Hundáková et al. (2014b)
Shaking (24 h, room temperature), $AgNO_3$, $Cu(NO_3)_2$, PE	Ver (Santa Luzia, Brazil)	*E. faecalis*	Broth dilution method, MIC determination, CFU counting	Hundáková et al. (2014a)

Cation exchange (stirring, 70–80 °C, 4–12h), $CuSO_4 \cdot 5H_2O$, reduction (Ar/H_2 atm. 500°C, 2 h) → Cu NPs	Sep – purified with HNO_3	*E. coli, S. aureus*	CFU counting	Esteban-Cubillo et al. (2006)
Cation exchange, $CuCl_2$, $ZnCl_2$, $NiCl_2$ → Cu_2O, ZnO, NiO NPs	Natural Zeol with 70wt.% Cli (the sedimentary deposit Zlatokop, Serbia) – Na^+-rich form	*E. faecalis*, *E. coli*, *P. caudatum*, *E. affinis*	CFU counting	Hrenovic et al. (2012)
Cation exchange (stirring 24 h, room temperature) $ZnCl_2$, $CuSO_4 \cdot 5H_2O$	Commercial Zeol X (Loyang Jianlong Chemical Industrial Co.)	*E. coli, P. aeruginosa, S. aureus, C. albicans, A. niger*	Disk diffusion method	Tekin and Bac (2016)
Ion exchange by melting, $CuSO_4 \cdot 5H_2O$, (550–560 °C, 10–90 min)	Ben (Na-Mt) (Rasht, Iran)	*E. coli, S. aureus*	CFU counting	Pourabolghasem et al. (2016)

nal permeability and proinflammatory cytokine in weanling pigs were investigated. Similar as in previous study, the weanling pigs (total 96 pigs with initial average weight 5.6 kg) were divided into four groups according the dietary treatments adjusted follows: (1) basal diet (control), (2) basal diet +1.5 g/kg Cu^{2+}-CaMt, (3) basal diet +1.5 g/kg Cu^{2+}-CaMt and (4) basal diet +75 mg/kg chlortetracycline. Experiment was carried out for 14 days. Results showed that diet with Cu^{2+}-Mt was as effective as chlortetracycline against diarrhea and inflammation, also improving intestinal microflora and mucosal barrier integrity of weanling pigs (Song et al. 2013).

The interesting study focused on potential use of Cu^{2+}-Mt in fish farming industry was also published. The effect of Cu^{2+}-Mt was studied on growth performance, microbial ecology and intestinal morphology of Nile tilapia (*Oreochromis niloticus*). The Nile tilapia (total 360 fingerlings with initial average weight 3.9 g) were divided into four groups according the dietary treatments adjusted follows: (1) basal diet, (2) basal diet +1.5 g/kg Mt, (3) basal diet +30 mg/kg $CuSO_4$ (with the Cu^{2+} equivalent to that in Cu^{2+}-Mt) and (4) basal diet +1.5 g/kg Cu^{2+}-Mt. Experiment was carried out for 56 days. The Cu^{2+}-Mt in diet improved growth performance, reduced the total intestinal aerobic bacterial counts and affected the composition of intestinal microflora in comparison with control and diet with Mt or $CuSO_4$. The composition of microflora was evaluated according the counts of *Aeromonas, Flavobacterium*, *Enterobacteriaceae*, *Vibrio*, *Pseudomonas*, *Acinetobacter*, *Alcaligence*, *Corynebactrium* and *Micrococcus* (Hu et al. 2007).

Antibacterial effect of Cu^{2+}-, Zn^{2+}-, Ag^{+}- and Ag^{0}- and cetylpyridinium (CP – exchanged Mt against *P. aeruginosa* (G^{-}) and *S. aureus* (G^{+}) was determined. Both bacteria are highly resistant to antibiotics and cause infections in hospitalized patients. The Ag^{+}-Mt, Cu^{2+}-Mt and Ag^{0}-Mt samples showed good antibacterial activity against both bacteria. The CP-Mt did not show antibacterial activity (Özdemir et al. 2010). The Ag-Mt, Cu-Mt and Zn-Mt were prepared by cation exchange of Mt. The antibacterial activity against *E. coli* (G^{-}), and antifungal activity against *P. cinnabarinus* and *P. ostreatus* were investigated. It was found that inhibition effect on *E. coli* decreased as Ag-Mt > Cu-Mt ≈ Zn-Mt. The inhibition effect on *P. cinnabarinus* decreased as Zn-Mt ≥ Cu-Mt > Ag-Mt. The inhibition effect on *P. ostreatus* decreased as Cu-Mt > Zn-Mt > Ag-Mt. The samples were as effective as the free Ag^{+} ions. The free Ag^{+}, Cu^{2+}, Zn^{2+} cations inhibited the bacterial and fungal growth in similar manner (Malachová et al. 2011).

The Cu NPs were synthetized on Mt substrate by in situ reduction of copper ammonium complex ion. As first, the Mt-$[Cu(NH_3)_4(H_2O)_2]^{2+}$ powder was prepared followed: $CuCl_2$ aqueous solution was made ammoniacal and copper ammonia complex ion $[Cu(NH_3)_4(H_2O)_2]^{2+}$ was formatted (indicating according a dark blue color) and Mt was added. The dried powder was suspended in ammoniacal water, the hydrazine hydrate wad added and stirred to a bluish purple color, washed and dried. The results showed that the Cu NPs were both intercalated and adsorbed by the Mt. Antibacterial activity of prepared material was studied on the G^{-} bacteria *E. coli* and *P. aeruginosa* and the G^{+} bacteria *S. aureus* and *E. faecalis*. Results showed mortality over 80% after 12 h of incubation. The MBC value of Cu NPs-Mt (Cu

NPs) determined for individual bacteria was 5.7 mg/mL (285 μg/ml) for *S. aureus*, 5.2 mg/mL (260 μg/ml) for *E. coli*, 5.1 mg/mL (255 μg/ml) for *E. faecalis*, 7.2 mg/mL (360 μg/ml) for *P. aeruginosa*. The antibacterial action of Cu NPs-Mt is based on Cu NPs/Cu ions mediated cell disruption which is aided by the Mt substrate which serves as a stable carrier for the Cu NPs and also increases the contact frequency with the bacterial cell. The cytotoxicity study performed on two human cells showed a decrease in viability in both cell lines. Nevertheless, the stabilizing effect was observed with increase of Cu NPs-Mt concentration (Bagchi et al. 2013).

The CuO NPs were synthetized on Mt substrate by thermal decomposition method. The CuO-Mt was prepared by adding of Na_2CO_3 and $CuSO_4$ to deionized water and stirred at 60 °C. Mt was added and suspension was stirred to forming green precipitate $Cu_4(SO_4)(OH)_6$, separated by filtration and kept to a muffle furnace at 600 °C. The mean diameter of small spherical CuO NPs agglomerated on Mt was determined as ~3–5 nm. The antibacterial test on *E. coli* (G^-) shows that the MIC values for samples Mt, CuO and CuO-Mt were 100, 10 and 0.1 ng, respectively. The results of disc susceptibility test show no antibacterial activity of Mt. Contrary, CuO and CuO-Mt show antibacterial behavior, and the inhibition zone was higher for CuO-Mt (Sohrabnezhad et al. 2014).

There are not many studies published on antibacterial activity of Cu^{2+} ions and Cu or CuO NPs on vermiculite as substrate.

The Cu-Ver was prepared by cation exchange and antibacterial activity was tested on *E. coli* (G^-). Moreover, in order to determine the influence of heating on the antibacterial activity, the Cu-Ver sample was heated at 200 or 400 °C. Results of halo test show good antibacterial activity of Cu-Ver and no significant decrease in activity of samples after heating (Li et al. 2002). The antibacterial and antiprotozoal effects of Ag^+, Cu^{2+} and Zn^{2+} cation exchanged in Mt and Ver were compared. Antibacterial activity was tested on the G^- bacterial strains *E. coli* and *P. aeruginosa* and the G^+ bacterial strain *E. faecalis*. Antiprotozoal effect was tested on *Trichomonas vaginalis* (*T. vaginalis*). Results show the high antibacterial and antiprotozoal effect. Moreover, it was found that *T. vaginalis* was the most sensitive on tested samples (Pazdziora et al. 2010).

Ver substrate was decorated with Cu NPs and antibacterial activity was studied against bacteria *S. aureus* (G^+). The Cu NPs were prepared by heat treatment and H_2 reduction. First, the Cu^{2+}-Ver samples were prepared by cation exchanged with $CuSO_4$ aqueous solution. Second, the Cu^{2+}-Ver were heat treated in a Lindberg hydrogen furnace filled with Ar. After achieved the reduction temperature 400 or 600 °C, the H_2 or air flow was introduced to the furnace. The Cu content in samples was from 1.7 to 3.5 wt.%. The size of Cu NPs distributed primarily on Ver surface was in the broad range from ~1 to 400 nm. The good antibacterial activity of prepared Cu NPs-Ver samples was confirmed (Drelich et al. 2011). The antibacterial activity of Ag-Ver, Cu-Ver and Ag,Cu-Ver materials was compared. The inhibition effect on bacterial growth was observed in all prepared Ag-, Cu-Ver samples. The synergic effect of Ag and Cu in combined samples was observed. Nevertheless, the antibacterial activity of samples contained Ag was better compared to samples contained Cu (Hundáková et al. 2013b, 2014a, b).

The antibacterial activity of Cu NPs prepared on *Zeol* mineral sepiolite was also studied. The Cu NPs on Sep were synthetized using the process of cation exchange with $CuSO_4$ aqueous solution and adjusting the pH with NaOH to precipitate the metallic cations. Then, the prepared powder was subjected to the reduction in a 90% Ar/10% H_2 atmosphere at 500 °C to obtain Cu NPs. The size of Cu NPs distributed on Sep was 2–5 nm. The antibacterial effect of Cu NPs-Sep was tested on *E. coli* (G^-) and *S. aureus* (G^+). The concentration of both bacteria was reduced about 99.99% after 24 h of action (Esteban-Cubillo et al. 2006). Hrenovic et al. (2012) compared antimicrobial activity of Cu_2O, ZnO and NiO NPs supported on natural Cli. The numbers of viable bacterial cells of *E. coli* and *S. aureus* were reduced for four to six orders of magnitude after 24 h contact with Cu_2O and ZnO NPs. Moreover, the Cu2O and ZnO NPs showed 100% of antiprotozoal activity against *Paramecium caudatum* (*P. caudatum*) and *Euplotes affinis* (*E. affinis*) after 1 h of contact. The antibacterial and antiprotozoal activity of NiO NPs was less efficient. The Cu^{2+}-Zeol and Zn^{2+}-Zeol materials were prepared from commercial Zeol by cation exchanged with $CuSO_4$ or $ZnCl_2$ aqueous solution. Moreover, the encapsulation of a fragrance molecule - triplal, was studied. The antimicrobial activity of materials before and after encapsulation was studied. The Cu^{2+}-Zeol and Zn^{2+}-Zeol inhibited the growth of *S. aureus* (G^+) more than the growth of *E. coli* (G^-) and *P. aeruginosa* (G^-). The Cu^{2+}-Zeol samples showed larger inhibition zone compared Zn^{2+}-Zeol against all bacteria. On the contrary, in antifungal activities test, the Zn^{2+}-Zeol samples showed larger inhibition zone compared Cu^{2+}-Zeol against yeast *Candida albicans* (*C. albicans*) and fungus *Aspergillus niger* (*A. niger*) (Tekin and Bac 2016).

14.2.3 Silver and Copper NPs on Carbon Materials

Nanostructured Graphite Oxide (GO) and low-cost GO coated with silver or sand nanoparticles were developed and characterized. Antibacterial efficacy of these nanoparticles was investigated using waterborne pathogenic *E. coli* strain. Inhibition of pathogenic *E. coli* with sand and GO NPs. Highest bacterial removal efficiency (100%) by the Coated Graphite Oxide and the lowest by sand filters with 17.9–88.9% reduction rate from 0 to 24 h, respectively. The filter system with GO composite can be used as an effective filter for water disinfection and production of potable and pathogens free drinking water (Jakobsen et al. 2011). GO based nanocomposites have raised significant interests in many different areas silver nanoparticle (AgNPs) anchored GO (GO-Ag) has shown promising antimicrobial potential. Factors affecting its antibacterial activity as well as the underlying mechanism remain unclear. GO-Ag nanocomposites with different Ag NPs to GO ratios examined for their antibacterial activities against both the G^- bacteria *E. coli* and the G^+ bacteria *S. aureus*. GO-Ag nanocomposite with an optimal ratio of AgNPs to GO is much more effective and shows synergistically enhanced, strong antibacterial activities at rather low dose (2.5 μg/ml) compare to pure AgNPs. The GO-Ag

nanocomposite is more toxic to *E. coli* than that to *S. aureus*. The antibacterial effects of GO-Ag nanocomposite are further investigated, revealing distinct, species-specific mechanisms. The results demonstrate that GO-Ag nanocomposite functions as a bactericide against the *E. coli* (G^-) through disrupting bacterial cell wall integrity, whereas it exhibits bacteriostatic effect on the *S. aureus* (G^+) by dramatically inhibiting cell division (Tang et al. 2013). The effect of bactericide dosage and pH on antibacterial activity of GO-Ag was examined. GO-Ag was much more destructive to cell membrane of *E. coli* than that of *S. aureus*. Experiments were carried out using catalase, superoxide dismutase and sodium thioglycollate to investigate the formation of reactive oxygen species and free silver ions in the bactericidal process. The activity of intracellular antioxidant enzymes was measured to investigate the potential role of oxidative stress. According to the consequence, synergetic mechanism including destruction of cell membranes and oxidative stress accounted for the antibacterial activity of GO-Ag nanocomposites. All the results suggested that GO-Ag nanocomposites displayed a good potential for application in water disinfection (Jones and Hoek 2010) (Fig. 14.7).

The combination of silver with copper gave enhanced result. Ag, Cu monometallic and Ag/Cu bimetallic NPs were in situ grown on the surface of graphene, which was produced by chemical vapor deposition using ferrocene as precursor and further functionalized to introduce oxygen-containing surface groups. The antibacterial performance of the resulting hybrids was evaluated against *E. coli* cells and compared experiments of varying metal type and concentration. It was found that both Ag- and Cu-based monometallic graphene composites significantly suppress bacterial growth, yet the Ag-based ones exhibit higher activity compared to that of their Cu-based counterparts. Compared with well-dispersed colloidal Ag NPs of the same metal concentration, Ag- and Cu-based graphene hybrids display weaker antibacterial activity. However, the bimetallic Ag/Cu NPs-graphene hybrids exhibit superior performance compared to that of all other materials tested, i.e., both the monometallic graphene structures as well as the colloidal NPs, achieving complete bacterial growth inhibition at all metal concentrations tested. A systematic analysis of antibacterial activity of GO nanosheets, Ag and Cu NPs, and combinations of Cu-Ag NPs, and GO-Cu-Ag nanocomposites against *E. coli*, *P. aeruginosa*, *S. aureus*, *K. pneumoniae* and Methicillin-resistant *S. aureus* (MRSA) was performed. MRSA showed highest resistance in all cases (Perdikaki et al. 2016; Jankauskaitė et al. 2016).

Transition metal NPs such as Ag and Cu have been grafted onto carbon nanotube surface through wet chemical approach leading to the development of densely packed NP decorated carbon nanotubes. Chemically active surface and high-temperature stability are the basic attributes to use carbon nanotubes as the template for the growth of NPs. The antimicrobial properties of acid-treated MWCNT (MWCNT-COOH), Ag-MWCNT, and Cu-MWCNT are investigated against *E. coli* (G^-) bacteria. Ag-MWCNT and Cu-MWCNT (97% kill vs. 75% kill), whereas MWCNT-COOH only killed 20% of bacteria. Possible mechanisms are proposed to explain the higher antimicrobial activity by NP-coated MWCNT. These findings suggest that

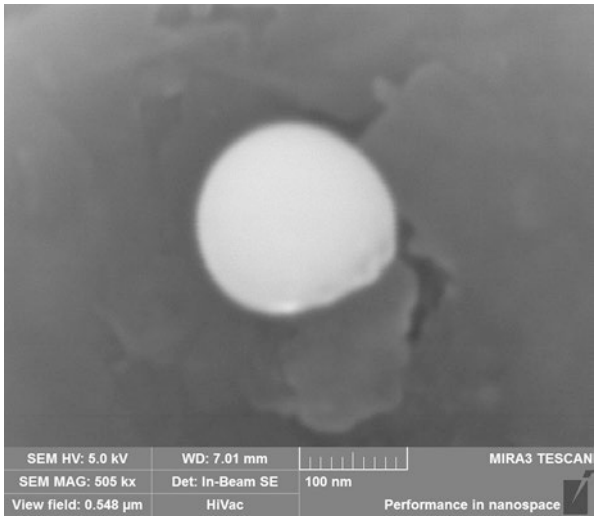

Fig. 14.7 Silver nanoparticle on graphite flake (SEM image acquired using secondary electron detector)

Ag-MWCNT and Cu-MWCNT may be used as effective antimicrobial materials that find applications in biomedical devices and antibacterial controlling system.

Ag NPs attached to CNTs have also shown enhanced activity against *E. coli*. Although, this strategy gives enhanced antibacterial effect but parameters like structural defects, agglomeration and impurities could also lead to partial loss in the ultimate expected results. Thus, precise control is required to further achieve the improved results. In the case of Ag-NPs attached to CNTs, it is believed that the antibacterial activity is due to Ag NPs. Several reports are available on the antibacterial activity of Ag NPs (Jones and Hoek 2010). When Ag-NPs are exposed to air, oxidation at the surface occurs (Eq. 14.1) and when in acidic environment, Ag^+ ions are released (Eq. 14.2) (Xiu et al. 2012). The released Ag^+ ions bind to the thiol group (SH) in enzymes and proteins on cellular surface and produce holes to enter the cell.

$$4\mathrm{Ag}(0) + \mathrm{O}_2 \rightarrow 2\mathrm{Ag}_2\mathrm{O} \tag{14.1}$$

$$\mathrm{Ag}_2\mathrm{O} + 4\mathrm{H}^+ \rightarrow 4\mathrm{Ag}^+ + 2\mathrm{H}_2\mathrm{O} \tag{14.2}$$

Another important aspect is the formation of Ag-NPs-CNT interface, which is believed to be quite stable without adversely affecting the antibacterial activity of Ag-NPs. In fact, presence of substrate (CNTs) serves two purposes in the experiment: (i) act as a host to increase the long term stability of NPs. Li et al. (2011) reported the long term stability for the about 1 month of MWCNTs and Ag-NPs composites. (ii) CNTs as possible substrates or a platform for drug delivery application. Yuan et al. (2008) showed the improvement of antibacterial efficiency against *S. aureus* (G^+) bacteria after the deposition of Ag-NPs on MWCNTs grafted with hyperbranched poly amidoamin (dMWCNTs), both d-MWNTs and d-MWNTs/Ag

were found equally effective against *E. coli* (G^-) and *P. aeruginosa* (G^-) bacteria. Jung et al. (2011) reported the antibacterial efficiency with pure MWCNTs, pure Ag-NPs and deposited Ag/CNTs against *E. coli* (G^-) and *S. epidermidis* (G^+), while higher inactivation of *E. coli* was observed relative to *S. epidermidis*. The present work dealt with the CVD growth of CNTs and synthesis of Ag-NPs and formation of composite by mixing CNTs in a mixture of $AgNO_3$ resorcinol and ethanol in one reaction.

14.3 Metal Oxides on Inorganic Substrates as Antimicrobial Agents

14.3.1 ZnO on Clay Minerals

Several studies dealing with preparation a characterization of nanocomposites where ZnO NPs are attached or bounded at clay matrix were published. Preparation of ZnO/Pal composites was developed by Huo and Yang (2010). Fibers of Pal were uniformly coated by ZnO NPs with average size equal to 15 nm. This composite exhibited antibacterial activity against *E. coli* (G^-) stronger than pure ZnO NPs. Authors proposed that clay matrix positively affected production of H_2O_2, which is harmful to living cells, and led to the cell membrane destruction and growth inhibition of bacteria. Zinc-enhanced montmorillonites were prepared and their influence to intestinal microbiota and barrier function in weaned pigs was evaluated (Jiao et al. 2015). Study revealed that providing 150 mg/kg Zn, supplementation prepared Zn-Mt improved postweaning diarrhea and enhanced growth performance in the weaned pigs. Explanation of results was attributed to the adsorption of the bacteria and immobilization on the surface of the composite. Alternatively, Zn was released from structure of the composite and directly exerted its antimicrobial effect on the bacteria. Therefore, the antibacterial effect of Zn-Mt may be explained by interactions of Mt with Zn. Also ZnO-Mt hybrid composite was investigated on performance, diarrhea, intestinal permeability and morphology (Hu et al. 2012). It was discovered that supplementing weaned pigs diets with 500 mg/kg of Zn from ZnO-Mt was as efficacious as 2,000 mg/kg of Zn from ZnO in promoting growth performance, alleviating diarrhea, improving intestinal microflora and barrier function. Pigs fed with 500 mg/kg of Zn from ZnO-Mt had higher performance and intestinal barrier function than those fed with Mt or 500 mg/kg of Zn from ZnO. ZnO-Mt composite was also tested as a material with potency to inhibit the cyanobacterial bloom (Gu et al. 2015). *Microcystis aeruginosa* (*M. aeruginosa*) is cyanobacteria which has a negative impact on water quality and therefore to human health. It was proved, that ZnO-Mt has strong flocculation effect on the tested cyanobacteria in comparison with pure Mt or ZnO under visible light and better photocatalytic degradation under UV irradiation. Synergistic effect of flocculation and photocatalysis of ZnO-Mt promoted removal of *M. aeruginosa*. Antibacterial activity of nanocomposite ZnO/

kaoline (ZinKa) was evaluated (Dědková et al. 2015a). ZinKa with 50 wt.% exhibited antibacterial activity under artificial day light against four common human pathogens (*S. aureus* (G^+), *E. faecalis* (G^+), *E. coli* (G^-), *P. aeruginosa* (G^-)). The highest antibacterial activity was observed against *S. aureus*, where the lowest value of MIC was determined equal to 0.41 mg/ml. As a comparison to this study, nanocomposite with the same chemical composition but prepared from different precursor and at slightly different conditions denoted Kao/ZnO (KAZN) was tested against the same four human pathogens at the same antibacterial assay (Dědková et al. 2016).

It was found that even chemical composition o ZinKa and KAZN is the same resulting antibacterial activity is different and therefore can be assumed that the way of preparation nanocomposites with clay matrix have an influence on resulting activity, nevertheless authors did not provide any detail explanation of this result because it needs to be investigated more. However, authors proposed possible mechanism of antibacterial activity, which could be based on photocatalytic reaction and production of ROS. Antimicrobial activity of ZnO-Ben composite was introduced by Pouraboulghasem et al. (2016). *E. coli* (G^-) served as a testing bacteria and pure Ben did not exhibit any antibacterial activity. After alkaline ion exchange treatment, antibacterial activity was observed. The most promising composite was ZnO/Ben after alkaline ion exchange for 60 and 90 min. Leaching test, which was also done, showed that ZnO/Ben did not present any risk to drinking water treatment due to the amount of leached zinc below to 4 mg/L, which is in the acceptable range according to World Health Organization regulations. Motshekga et al. (2013) published study dealing with composites where ZnO, Ag and combination of Ag- ZnO NPs supported on Ben clay were prepared. Disc diffusion method was used as a method for antibacterial assay where *E. coli* (G^-) with *E. faecalis* (G^+) were selected as tested bacteria. ZnO-clay composite and Ag-clay composite exhibited antibacterial activity however Ag/ZnO-clay exhibited the highest antibacterial activity from tested composites and according to authors it could be used as a material for drinking water treatment to target the G^+ also the G^- bacteria.

14.3.2 TiO_2 on Clay Minerals

There are many published papers dealing with photocatalytic activity of TiO_2/clay based nanocomposites, however, only a few are dealing with the antibacterial activity or describing possible applications in medicine. Kao/TiO_2 (KATI) nanocomposite was prepared and antibacterial activity in relation to irradiation time was investigated (Dědková et al. 2014). A standard microdilution test was used to determine the antibacterial activity using four human pathogenic bacterial strains (*S. aureus* (G^+), *E. coli* (G^-), *E. faecalis* (G^+), *P. aeruginosa* (G^-)). Artificial day light was applied to induce photocatalytic reaction. It was observed that UV light is not essential for antibacterial activity of KATI composite which is important in terms of potential applications for antibacterial modification of various surfaces.

Authors proposed that these nanocomposites would be used in future e.g. for surface treatment of external fixators in the treatment of complicated fractures of humans or animals for reduction of potential infection. TiO_2 nanotubes loaded with ZnO and Ag NPs were investigated by Roguska et al. (2015) with respect functional coatings to enhance bio-compatibility and antibacterial activity of implant materials. Authors observed considerable antibacterial activity of pure TiO_2 nanotubes to *S. epidermidis* (G^+), however, loading of nanotubes with nanoparticles significantly increased its effect on tested bacteria, where cell viability and adhesion extenuated after 1.5 h contact with modified surface. This functional coating seems to be promising delivery system to reduce bone implant related infections after operations; nevertheless, the amount of loaded nanoparticles has to be balanced to avoid overdose and potential risk to patients.

14.3.3 ZnO on Carbon Materials

Different forms of carbon may serve as a matrix for anchoring of nanoparticles. Simple hydrothermal method was used for decoration of graphene sheets with ZnO NPs (Bykkam et al. 2015). *S. typhi* (G^-) and *E. coli* (G^-) were used during well diffusion test to evaluate the antibacterial activity of prepared composite material. Provided results shown that few layered graphene sheets decorated by ZnO NPs exhibited good antibacterial activity. ZnO:Cu:Graphene nanopowder and its photocatalytic and antibacterial activity was studied (Ravichandran et al. 2016). It was demonstrated that this material has better photocatalytic and antibacterial properties in comparison with pure ZnO and ZnO:Cu nanopowders. Authors proposed that graphene layers could efficiently separate the photoinduced charge carriers and delay their recombination. This material is potential candidate not only in the field of decontamination of organic pollutants but also in medicine as an effective antibacterial agent. Plasmonic sulfonated graphene oxide-ZnO-Ag (SGO-ZnO-Ag) composites were developed by Gao et al. (2013) via nanocrystal-seed-directed hydrothermal method. Surface plasmon resonance of Ag shifted the light absorption ability of this material to visible region of spectra. Moreover, hierarchical structure of SGO-ZnO-Ag improved the incident light scattering and reflection. Finally, sulfonated graphite sheets enabled charge transfer and reduce the recombination of electron-hole pairs. These synergistic effects led to much faster rate of photodegradation of Rhodamine B and disinfection of *E. coli* than in the case of pure ZnO. SGO-ZnO-Ag composite is promising candidate in the field of disinfection and photodegradation. Dědková et al. (2015c) introduced nanostructured composite material ZnO/graphite (ZnGt). Micromilled and high purity natural graphite (Gt) were used as a matrix to anchoring of NPs, where 50 wt.% of ZnO NPs were given. Antibacterial assay using four human pathogens showed that ZnGt composited exhibited antibacterial activity under artificial daylight irradiation. Those materials could find the potential application in the field of surface modification of materials

used in medicine especially when UV light is not essential for induction of its antibacterial activity.

Carbon fibers may also serve as a material for anchoring of NPs, however, it is still not frequently studied. Carbon nanofibers decorated with TiO_2/ZnO NPs were prepared via electrospinning method by Pant et al. (2016). The small amount of ZnO was introduced to fibers through electrospinning and that provided nucleation sites for the crystal growth of ZnO during hydrothermal synthesis and enabled holding of TiO_2/ZnO particles on the fiber surface. This process of preparation provided composite material with better stability. Antibacterial activity of the prepared material was tested against *E. coli* under UV irradiation. It was demonstrated that carbon-TiO_2/ZnO has higher antibacterial activity than TiO_2/ZnO. This material is promising for air and water purification purposes (Pant et al. 2013).

Carbon nanotubes are being studying intensively in terms of potential applications in several fields of human lives. Antimicrobial properties of carbon nanotubes were already published (Liu et al. 2009) and currently surface modifications and functionalization of carbon nanotubes are investigated. Metal and metal oxides based nanoparticles may serve as one of many possible modificants. ZnO coated multi-walled carbon nanotubes (ZnO/MWCNTs) prepared by Sui et al. (2013) were tested in terms of potential antimicrobial material. *E. coli* was selected as a target organism. Raw and purified MWCNTs were used as a reference material. Obtained results indicate that raw and purified MWCNTs only adsorbed cells of *E. coli*, whereas ZnO/MWCNTs showed bactericidal effect. In other study functionalized multi-walled carbon nanotubes in ZnO thin films (MWCNT-ZnO) were synthesized for photoinactivation of bacteria (Akhavan et al. 2011). MWCNT–ZnO nanocomposite thin films with various MWCNT contents were prepared. Photoinactivation of *E. coli* under UV-visible light irradiation on the surface of unfuctionalized film as well as on the surface of MWCNT–ZnO functionalized film was observed, where functionalized composites with various MWCNT content showed significantly higher photoiactivation of bacteria. Result showed that 10% of MWCNT-ZnO is the optimum content in the film. Proposed mechanism of the antibacterial activity is assigned to charge transfer through Zn-O-C bonds, which are originated, between atoms of zinc of ZnO film and oxygen atoms of carboxylic functional groups of the MWCNTs.

14.3.4 TiO_2 on Carbon Materials

Direct redox reaction served a method for preparation of composites of ultrafine TiO_2 nanoparticles and graphene sheets (TiO_2/GSs) (Cao et al. 2013). The composite possessed extended light absorption, which means that the composite could be excited by visible light. Antibacterial potency induced via visible-light irradiation was investigated against *E. coli*. Results shown, that the antibacterial activity of TiO_2/GSs was significantly higher than to pure TiO_2 nanoparticles. Authors proposed possible application of this material in the field of indoor air disinfection. Titanium dioxide-reduced graphene oxide (TiO_2-RGO) were synthesized by the

photocatalytic reduction of exfoliated graphene oxide (GO) by TiO_2 under UV irradiation in the presence of methanol as a hole acceptor (Fernández-Ibáñez et al. 2015). Water contaminated with *E. coli* and *Fusarium solani* (*F. solani*) was treated by TiO_2-RGO and P25 (TiO_2) under real sunlight. Fast disinfection of the contaminated water was observed. Inactivation of *F. solani* was similar for both tested materials; nevertheless, the higher inactivation of *E. coli* was caused by TiO_2-RGO composite. Proposed explanation is given to the production of singlet oxygen via visible light excitation of the composite. Another study was focused on the magnetic graphene oxide–TiO_2 (MGO–TiO_2) (Chang et al. 2015) composites and its antibacterial activity against *E. coli* under solar irradiation. It was observed that MGO–TiO_2 caused complete inaction of the *E. coli* within 30 min under solar irradiation.

Graphene oxide-TiO_2-Ag (GO-TiO_2-Ag) composites were introduced as highly efficient water disinfectants by Liu et al. (2013). Antibacterial activity of GO-TiO_2 and GO-Ag against *E. coli* was observed, however, the highest activity showed GO-TiO_2-Ag composite. The explanation is given to enhanced photocatalytic reaction, which led to bacterial inactivation. It is expected that Ag nanoparticles significantly suppress recombination of photoinduced electrons and holes, which enhance the photocatalytic performance of GO-TiO_2-Ag nanocomposites. Simple one step hydrothermal reaction of TiO_2 nanoparticles (Degusa P25) with $AgNO_3$ and reduced graphene oxide led to creation of multifunctional Ag-TiO_2/rGO composite (Pant et al. 2016). Enhanced optical response of the nanocomposite led to the absorption of light in the visible spectrum via localized surface plasmon resonance effects. Antibacterial activity was performed on *E. coli* as a tested organism. The nanocomposite showed synergistic effect of photocatalytic disinfection of E. coli than pure TiO_2 or TiO_2-Ag and therefore its antibacterial activity was significantly higher. It seems that Ag-TiO_2/rGO is a promising candidate for water treatment due to its improved photocatalytic and antibacterial properties. One study introduced nanostructured composite material graphite/TiO_2 (GrafTi) (Dědková et al. 2015c) and its antibacterial activity against four common human pathogens (*S. aureus* (G^+), *E. coli* (G^-), *E. faecalis* (G^+), *P. aeruginosa* (G^-)) under artificial day light. Antibacterial activity of this material is attributed to photocatalytic reaction with subsequent interaction of ROS with bacterial cells. Difference between antibacterial activity against selected bacteria and difference in the onset of activity were observed. The developed nanocomposite exhibited a potential for future applications as antibacterial agents for modification of surfaces to control bacterial growth e.g. in biomedical fields.

Nanocomposites based on TiO_2 nanoparticles and various amounts of functionalized MWCNTs (TiO_2-MWCNTs) were synthesized (Koli et al. 2016) and its antibacterial activity against *E. coli* and *S. aureus* under artificial visible light irradiation has been performed. Experiments revealed high antibacterial activity of TiO_2-MWCNTs, while bare TiO_2 nanoparticles did not show any inhibitory effect. Authors expect that it is caused by smaller particle size and visible light activation; however, detail explanation is not provided. This material is efficient against wide range of bacteria and may be used to control the persistence and spreading of bacterial infections.

14.4 Conclusion

Various types of antimicrobial materials are researched and developed based on both inorganic and organic matter. One of them are purely inorganic based on inorganic substrate and enhanced by metals or metal oxides. Clay minerals are suitable substrates for various metals as silver, copper their oxides or oxides of zinc or titanium. Improved and more stable antimicrobial action is proven for wide range of bacterial strains, and anchored interaction in hybrids provides lower mobility of nanoparticles therefore lowered negative effect on environment. Similar interaction is observed in case of carbon materials (nanocarbons), however, the forces attracting the active particles are non-bonding interactions. Utilization of such hybrid antimicrobial materials are very wide. There are applications in packaging using those particles as nanofillers for polymeric nanocomposites or medicinal application, where active particles anchored on clay or carbon substrate can be promising delivery system to reduce bone implant related infections after operations, for surface treatment of external fixators in the treatment of complicated fractures of humans or animals for reduction of potential infection or dental applications. They can be used for waste water treatment and sanitary purposes as well. However, the application of antimicrobial materials should be carefully tailored and the toxicity effect considered.

Acknowledgement This chapter was created with support of the Project No. LO1203 "Regional Materials Science and Technology Centre – Feasibility Program" funded by Ministry of Education, Youth and Sports of the Czech Republic and by the MSMT (SP2016/75 and SP2017/86).

References

Akhavan O, Azimirad R, Safa S. Functionalized carbon nanotubes in ZnO thin films for photoinactivation of bacteria. Mater Chem Phys. 2011;130(1–2):598–602.

Bagchi B, Kar S, Dey SK, Bhandary S, Roy D, Mukhopadhyay TK, et al. In situ synthesis and antibacterial activity of copper nanoparticle loaded natural montmorillonite clay based on contact inhibition and ion release. Colloid Surf B-Biointerfaces. 2013;108:358–65.

Baker C, Pradhan A, Pakstis L, Pochan DJ, Shah SI. Synthesis and antibacterial properties of silver nanoparticles. J Nanosci Nanotechnol. 2005;5:244–9.

Benaliouche F, Hidous N, Guerza M, Zouad Y, Boucheffa Y. Characterization and water adsorption properties of Ag and Zn-exchanged A zeolites. Microporous Mesoporous Mater. 2015;209:184–8.

Braydich-Stolle L, Hussain S, Schlager J, Hofmann MC. In vitro cytotoxicity of nanoparticles in mammalian germ line stem cells. Toxicol Sci. 2005;88:412–9.

Brigatti MF, Galan E, Theng BKG. Structures and mineralogy of clay minerals. In: Bergaya F, Theng BKG, Lagaly G, editors. Handbook of clay science. Oxford: Elsevier; 2006. p. 19–86.

Bykkam S, Narsingam S, Ahmadipour M, Dayakar T, et al. Few layered graphene sheet decorated by ZnO nanoparticles for anti-bacterial application. Superlattice Microst. 2015;83:776–84.

Cao B, Cao S, Dong P, Gao J, Wang J. High antibacterial activity of ultrafine TiO_2/graphene sheets nanocomposites under visible light irradiation. Mater Lett. 2013;93:349–52.

Cao GF, Sun Y, Chen JG, Song LP, Jiang JQ, Liu ZT, Liu ZW. Sutures modified by silver-loaded montmorillonite with antibacterial properties. Appl Clay Sci. 2014;93-94:102–6.
Cataldo F, Da Ros T. Medicinal chemistry and pharmacological potential of fullerenes and carbon nanotubes. Trieste: Springer; 2008.
Chang YN, Zhang M, Xia L, Zhang J, Xing G. The toxic effects and mechanisms of CuO and ZnO nanoparticles. Materials. 2012;5:2850–71.
Chang Y, Ou X, Zeng G, Gong J, Deng C. Synthesis of magnetic graphene oxide-TiO_2 and their antibacterial properties under solar irradiation. Appl Surf Sci. 2015;343:1–10.
Chung CJ, Su CW, He JL. Antimicrobial efficacy of photocatalytic TiO2 coatings prepared by arc ion plating. Surf Coat Technol. 2007a;202(4–7):1302–7.
Chung CJ, Su CW, He JL. Microstructural effect on the antimicrobial efficacy of arc ion plated TiO_2. J Mater Res. 2007b;22:3137–43.
Chung CJ, Lin HI, Hsieh PY, Chen KC, He JL, Leyland A, et al. Growth behavior and microstructure of arc ion plated titanium dioxide. Surf Coat Technol. 2009;204:915–22.
Chung CJ, Tsou HK, Chen HL, Hsieh PY, He JL. Low temperature preparation of phase-tunable and antimicrobial titanium dioxide coating on biomedical polymer implants for reducing implant-related infections. Surf Coat Technol. 2011;205:5035–9.
Copcia VE, Luchian C, Dunca S, Bilba N, Hristodor CM. Antibacterial activity of silver-modified natural clinoptilolite. J Mater Sci. 2011;46:7121–8.
Costa C, Conte A, Buonocore GG, Del Nobile MA. Antimicrobial silver-montmorillonite nanoparticles to prolong the shelf life of fresh fruit salad. Int J Food Microbiol. 2011;148:164–7.
Costa C, Conte A, Buonocore GG, Lavorgna M, Del Nobile MA. Calcium-alginate coating loaded with silver-montmorillonite nanoparticles to prolong the shelf-life of fresh-cut carrots. Food Res Int. 2012;48:164–9.
Dankovich TA, Smith JA. Incorporation of copper nanoparticles into paper for point-of-use water purification. Water Res. 2014;63:245–51.
Dědková K, Matějová K, Lang J, Peikertová P, Mamulová Kutláková K, Neuwirthová L, et al. Antibacterial activity of kaolinite/nanoTiO_2 composites in relation to irradiation time. J Photochem Photobiol B Biol. 2014;135:17–22.
Dědková K, Janíková B, Matějová K, Peikertová P, Neuwirthová L, Holešinský J, Kukutschová J. Preparation, characterization and antibacterial properties of ZnO/kaoline nanocomposites. J Photochem Photobiol B Biol. 2015a;148:113–7.
Dědková K, Lang J, Matějová K, Peikertová P, Holešinsky J, Vodárek V, et al. Nanostructured composite material graphite/TiO_2 and its antibacterial activity under visible light irradiation. J Photochem Photobiol B-Biol. 2015b;149:265–71.
Dědková K, Janíková B, Matějová K, Čabanová K, Váňa R, Kalup A, et al. ZnO/graphite composites and its antibacterial activity at different conditions. J Photochem Photobiol B Biol. 2015c;151:256–63.
Dědková K, Mamulová Kutlákova K, Matějová K, Kukutschová J. The study of the antibacterial activity of kaolinite/ZnO composites. Adv Sci Lett. 2016;22(3):695–8.
Deryabin DG, Davydova OK, Yankina ZZ, Vasilchenko AS, Miroshnikov SA, Kornev AB, et al. The activity of [60] fullerene derivatives bearing amine and carboxylic solubilizing groups against *Escherichia coli*: a comparative study. J Nanomater. 2014;2014:1–9.
Drelich J, Li B, Bowen P, Hwang JY, Mills O, Hoffman D. Vermiculite decorated with copper nanoparticles: novel antibacterial hybrid material. Appl Surf Sci. 2011;257:9435–43.
Esteban-Cubillo A, Pecharromán C, Aguilar E, Santarén J, Moya JS. Antibacterial activity of copper monodispersed nanoparticles into sepiolite. J Mater Sci. 2006;41:5208–12.
Feng QL, Wu J, Chen GQ, Cui FZ, Kim TN, Kim JO. A mechanistic study of an antibacterial effect of silver ions on *Escherichia coli* and *Staphylococcus aureus*. J Biomed Mater Res. 2000;662–8.
Fernández-Ibáñez P, Polo-López MI, Malato S, Wadhwa S, Hamilton JWJ, Dunlop PSM, et al. Solar photocatalytic disinfection of water using titanium dioxide graphene composites. Chem Eng J. 2015;261:36–44.

Gao P, Ng K, Sun DD. Sulfonated graphene oxide-ZnO-Ag photocatalyst for fast photodegradation and disinfection under visible light. J Hazard Mater. 2013;262:826–35.

Girase B, Depan D, Shah JS, Xu W, Misra RDK. Silver–clay nanohybrid structure for effective and diffusion-controlled antimicrobial activity. Mater Sci Eng C. 2011;31:1759–66.

Gu N, Gao J, Wang K, Yang X, Dong W. ZnO-montmorillonite as photocatalyst and flocculant for inhibition of cyanobacterial bloom. Water Air Soil Pollut. 2015;226(5):136–47.

Guerra R, Lima E, Viniegra M, Guzman A, Lara V. Growth of *Escherichia coli* and *Salmonella typhi* inhibited by fractal silver nanoparticles supported on zeolites. Microporous Mesoporous Mater. 2012;147:267–73.

Gurr JR, Wang ASS, Chen CH, Jan KY. Ultrafine titanium dioxide particles in the absence of photoactivation can induce oxidative damage to human bronchial epithelial cells. Toxicology. 2005;213(1–2):66–73.

Hashimoto K, Irie H, Fujishima A. TiO_2 photocatalysis: a historical overview and future prospects. Jpn J Appl Phys. 2005;44(12):8269–85.

Holtz RD, Lima BA, Souza Filho AG, Brocchi M, Alves OL. Nanostructured silver vanadate as a promising antibacterial additive to water-based paints. Nanomed-Nanotechnol Biol Med. 2012;8:935–40.

Hrenovic J, Milenkovic J, Daneu N, Matonickin Kepcija R, Rajic N. Antimicrobial activity of metal oxide nanoparticles supported onto natural clinoptilolite. Chemosphere. 2012;88:1103–7.

Hrenovic J, Milenkovic J, Goic-Barisic I, Rajic N. Antibacterial activity of modified natural clinoptilolite against clinical isolates of *Acinetobacter baumannii*. Microporous Mesoporous Mater. 2013;169:148–52.

Hu CH, Xia MS. Adsorption and antibacterial effect of copper-exchanged montmorillonite on *Escherichia coli* K88. Appl Clay Sci. 2006;31:180–4.

Hu CH, Xu ZR, Xia MS. Antibacterial effect of Cu^{2+}-exchanged montmorillonite on *Aeromonas hydrophila* and discussion on its mechanism. Vet Microbiol. 2005;109:83–8.

Hu CH, Xu Y, Xia MS, Xiong L, Xu ZR. Effects of Cu^{2+}-exchanged montmorillonite on growth performance, microbial ecology and intestinal morphology of Nile tilapia (*Oreochromis niloticus*). Aquaculture. 2007;270:200–6.

Hu CH, Gu LY, Luan ZS, Song J, Zhu K. Effects of montmorillonite-zinc oxide hybrid on performance, diarrhea, intestinal permeability and morphology of weanling pigs. Anim Feed Sci Technol. 2012;177:108–15.

Hundáková M, Valášková M, Pazdziora E, Matějová K, Študentová S. Structural and antibacterial properties of original vermiculite and acidified vermiculite with silver. In: Proceedings of the 3rd International Conference NANOCON 2011; 2011 Sep 21–23; Brno, CZ; Ostrava: Tanger Ltd, 2011. p. 617–22.

Hundáková M, Valášková M, Seidlerová J, Pazdziora E, Matějová K. Preparation and evaluation of different antibacterial Ag-montmorillonites. In: Proceedings of the 4th International Conference NANOCON 2012; 2012 Oct 23–25; Brno, CZ. Ostrava: Tanger Ltd; 2013a. p. 591–5.

Hundáková M, Valášková M, Tomášek V, Pazdziora E, Matějová K. Silver and/or copper vermiculites and their antibacterial effect. Acta Geodyn Geomater. 2013b;10(1):97–104.

Hundáková M, Valášková M, Samlíková M, Pazdziora E. Vermiculite with Ag and Cu used as an antibacterial nanofiller in polyethylene. GeoSci Eng. 2014a;LX(3):28–39.

Hundáková M, Valášková M, Seidlerová J. Stability of silver and copper on clay minerals in water and their antibacterial activity. In: Proceedings of the 5th International Conference NANOCON 2013; 2013 Oct 16–18; Brno, CZ; Ostrava: Tanger Ltd; 2014b. p. 632–7.

Hundáková M, Simha Martynková G, Valášková M, Měřínská D, Pazdziora E. Antibacterial polypropylene/Ag-kaolinite, preparation and characterization. Adv Sci Lett. 2016;22(3):656–60.

Huo C, Yang H. Synthesis and characterization of ZnO/palygorskite. Appl Clay Sci. 2010;50(3):362–6.

Jakobsen L, Andersen AS, Friis-Møller A, Jørgensen B, Krogfelt KA, Frimodt-Møller N. Silver resistance: an alarming public health concern? Int J Antimicrob Agents. 2011;38(5):454–5.

Jankauskaitė V, Vitkauskienė A, Lazauskas A, Baltrusaitis J, Prosyčevas I, Andrulevičius M. Bactericidal effect of graphene oxide/Cu/Ag nanoderivatives against *Escherichia coli*,

Pseudomonas aeruginosa, *Klebsiella pneumoniae*, *Staphylococcus aureus* and methicillin-resistant *Staphylococcus aureus*. Int J Pharm. 2016;511(1):90–7.
Jiao LF, Ke YL, Xiao K, Song ZH, Lu JJ, Hu CH. Effects of zinc-exchanged montmorillonite with different zinc loading capacities on growth performance, intestinal microbiota, morphology and permeability in weaned piglets. Appl Clay Sci. 2015;113:40–3.
Johari SA, Kalbassi MR, Soltani M, Yu IJ. Application of nanosilver-coated zeolite as water filter media for fungal disinfection of rainbow trout (*Oncorhynchus mykiss*) eggs. Aquacult Int. 2016;24:23–38.
Jones CM, Hoek EMV. A review of the antibacterial effects of silver nanomaterials and potential implications for human health and the environment. J Nanopart Res. 2010;12:1531–51.
Jones N, Ray B, Ranjit KT, Manna AC. Antibacterial activity of ZnO nanoparticle suspensions on a broad spectrum of microorganisms. FEMS Microbiol Lett. 2008;279(1):71–6.
Jung JH, Hwang GB, Lee JE, Bae GN. Preparation of airborne Ag/CNT hybrid nanoparticles using an aerosol process and their application to antimicrobial air filtration. Langmuir. 2011;27:10256–64.
Karel FB, Koparal AS, Kaynak E. Development of silver ion doped antibacterial clays and investigation of their antibacterial activity. Adv Mater Sci Eng. 2015;2015:1–6. ID: 409078
Kawahara K, Tsuruda K, Morishita M, Uchida M. Antibacterial effect of silver-zeolite on oral bacteria under anaerobic conditions. Dent Mater. 2000;16:452–5.
Kheiralla ZMH, Rushdy AA, Betiha MA, Yakob NAN. High-performance antibacterial of montmorillonite decorated with silver nanoparticles using microwave assisted method. J Nanopart Res. 2014;16:2560.
Kokura S, Handa O, Takagi T, Ishikawa T, Naito Y, Yoshikawa T. Silver nanoparticles as a safe preservative for use in cosmetics. Nanomed-Nanotechnol Biol Med. 2010;6:570–4.
Koli VB, Dhodamani AG, Raut AV, Thorat ND, Pawar SH, Delekar SD. Visible light photoinduced antibacterial activity of TiO_2-MWCNTs nanocomposites with varying the contents of MWCNTs. J Photochem Photobiol A-Chem. 2016;328:50–8.
Kollef MH, Afessa B, Anzueto A, Veremakis C, Kerr KM, Margolis BD, et al. Silver coated endotracheal tubes and incidence of ventilator-associated pneumonia. JAMA. 2008;300(7):805–13.
Li B, Yu S, Hwang JY, Shi S. Antibacterial vermiculite nano-material. J Minerals Mater Charact Eng. 2002;1:61–8.
Li Z, Fan L, Zhang T, Li K. Facile synthesis of Ag nanoparticles supported on MWCNTs with favorable stability and their bactericidal properties. J Hazard Mater. 2011;187:466–72.
Liu S, Wei L, Hao L, Fang N, Chang MW, Xu R, et al. Sharper and faster 'nano darts' kill more bacteria: a study of antibacterial activity of individually dispersed pristine single-walled carbon nanotube. ACS Nano. 2009;3(12):3891–902.
Liu S, Keong A, Xu R, Wei J, Tan CM, Yanga Y, Chen Y. Antibacterial action of dispersed single-walled carbon nanotubes on *Escherichia coli* and *Bacillus subtilis* investigated by atomic force microscopy. Nanoscale. 2010;2:2744.
Liu S, Zeng TH, Hofmann M, Burcombe E, Wei J, Jiang R, et al. Antibacterial activity of graphite, graphite oxide, graphene oxide, and reduced graphene oxide: membrane and oxidative stress. ACS Nano. 2011;5(9):6971–80.
Liu L, Bai H, Liu J, Sun DD. Multifunctional graphene oxide-TiO_2-Ag nanocomposites for high performance water disinfection and decontamination under solar irradiation. J Hazard Mater. 2013;261:214–23.
Lok CN, Ho CM, Chen R, He QY, Yu WY, Sun H, et al. Proteomic analysis of the mode of antibacterial action of silver nanoparticles. J Proteome Res. 2006;5:916–24.
Lu W, Senapati D, Wang S, Tovmachenko O, Kumar Singh A, Hongtao Y, et al. Effect of surface coating on the toxicity of silver nanomaterials on human skin keratinocytes. Chem Phys Lett. 2010;487:92–6.
Maeda K. Basic studies on possible clinical application of antibacterial zeolite. Nesshou. 1987;13:316–21.
Magaña SM, Quintana P, Aguilar DH, Toledo JA, Ángeles-Chávez C, Cortés MA, et al. Antibacterial activity of montmorillonites modified with silver. J Mol Catal A-Chem. 2008;281:192–9.

Malachová K, Praus P, Pavlíčková Z, Turicová M. Activity of antibacterial compounds immobilised on montmorillonite. Appl Clay Sci. 2009;43:364–8.

Malachová K, Praus P, Rybková Z, Kozák O. Antibacterial and antifungal activities of silver, copper and zinc montmorillonites. Appl Clay Sci. 2011;53(4):642–5.

Martynková GS, Valášková M. Antimicrobial nanocomposites based on natural modified materials: a review of carbons and clays. J Nanosci Nanotechnol. 2014;14(1):673–93.

Meghana S, Kabra P, Chakraborty S, Padmavathy N. Understanding the pathway of antibacterial activity of copper oxide nanoparticles. RSC Adv. 2015;5:12293–9.

Miyoshi H, Ohno H, Sakai K, Okamura N, Kourai H. Characterization and photochemical and antibacterial properties of highly stable silver nanoparticles prepared on montmorillonite clay in n-hexanol. J Colloid Interface Sci. 2010;345:433–41.

Mizuno K, Zhiyentayev T, Huang L, Khalil S, Nasim F, Tegos GP, et al. Antimicrobial photodynamic therapy with functionalized fullerenes: quantitative structure-activity relationships. J Nanomed Nanotechnol. 2011;2(2):1–9.

Motshekga SC, Ray SS, Onyango MS, Momba MNB. Microwave-assisted synthesis, characterization and antibacterial activity of Ag/ZnO nanoparticles supported bentonite clay. J Hazard Mater. 2013;262:439–46.

Narayan RJ, Abernathy H, Riester L, Berry CJ, Brigmon R. Antimicrobial properties of diamond-like carbon-silver-platinum nanocomposite thin films. J Mater Eng Perform. 2005;14:435–40.

Özdemir G, Limoncu MH, Yapar S. The antibacterial effect of heavy metal and cetylpridinium-exchanged montmorillonites. Appl Clay Sci. 2010;48:319–23.

Panáček A, Kvítek L, Prucek R, Kolář M, Večeřová R, Pizúrová N, et al. Silver colloid nanoparticles: synthesis, characterization, and their antibacterial activity. J Phys Chem. 2006;110:16248–53.

Pant B, Raj H, Barakat NAM, Park M, Jeon K. Carbon nanofibers decorated with binary semiconductor (TiO_2/ZnO) nanocomposites for the effective removal of organic pollutants and the enhancement of antibacterial activities. Ceram Int. 2013;39(6):7029–35.

Pant B, Singh P, Park M, Park S, Kim H. General one-pot strategy to prepare Ag- TiO_2 decorated reduced graphene oxide nanocomposites for chemical and biological disinfectant. J Alloys Compd. 2016;671:51–9.

Parolo ME, Fernández LG, Zajonkovsky I, Sánchez MP, Baschini M. Antibacterial activity of materials synthesized from clay minerals. In: Méndez-Vilas A, editor. Science against microbial pathogens: communicating current research and technological advances, vol. 1: FORMATEX; 2011. p. 144–51. ISBN-13: 978-84-939843-1-1.

Pazdziora E, Matějová K, Valášková M, Holešová S, Hundáková M. Comparison of antibacterial and antiprotozoal effects of nanoparticles Zn^{2+}, Cu^{2+} a Ag^{+} intercalated on clay minerals. In: Proceedings of the 2nd International Conference NANOCON 2010; 2010 Oct 12–14; Olomouc, CZ; Ostrava: Tanger Ltd; 2010. p. 460–4.

Perdikaki A, Galeou A, Pilatos G, Karatasios I, Kanellopoulos KH, Prombona A, Karanikolos GN. Ag and Cu monometallic and Ag/Cu bimetallic nanoparticle–graphene composites with enhanced antibacterial performance. ACS Appl Mater Interfaces. 2016;8(41):27498–510.

Pourabolghasem H, Ghorbanpour M, Shayegh R. Antibacterial activity of copper-doped montmorillonite nanocomposites prepared by alkaline ion exchange method. J Phys Sci. 2016;27(2):1–12.

Pouraboulghasem H, Ghorbanpour M, Shayegh R, Lotfiman S. Synthesis, characterization and antimicrobial activity of alkaline ion-exchanged ZnO/bentonite nanocomposites. J Cent South Univ. 2016;23(4):787–92.

Rai VR, Bai AJ. Nanoparticles and their potential application as antimicrobials. In: Méndez-Vilas A, editor. Science against microbial pathogens: communicating current research and technological advances. Badajoz: FORMATEX; 2011. p. 197–209.

Rai M, Yadav A, Gade A. Silver nanoparticles as a new generation of antimicrobials. Biotechnol Adv. 2009;27:76–83.

Ravichandran K, Chidhambaram N, Gobalakrishnan S. Copper and graphene activated ZnO nanopowders for enhanced photocatalytic and antibacterial activities. J Phys Chem Solids. 2016;93:82–90.

Rivera-Garza M, Olguín MT, García-Sosa I, Alcántara D, Rodríguez-Fuentes G. Silver supported on natural Mexican zeolite as an antibacterial material. Microporous Mesoporous Mater. 2000;39:431–44.

Roguska A, Belcarz A, Pisarek M, Ginalska G, Lewandowska M. TiO_2 nanotube composite layers as delivery system for ZnO and Ag nanoparticles – an unexpected overdose effect decreasing their antibacterial efficacy. Mater Sci Eng C Mater Biol Appl. 2015;51:158–66.

Rosa-Gomez de la I, Olguina MT, Alcantara D. Antibacterial behavior of silver-modified clinoptilolite-heulandite rich tuff on coliform microorganisms from wastewater in a column system. J Environ Manag. 2008;88:853–63.

Rosa-Gomez de la I, Olguina MT, Alcantara D. Silver-modified mexican clinoptilolite-rich tuffs with various particle sizes as antimicrobial agents against *Escherichia coli*. J Mex Chem Soc. 2010;54(3):139–42.

Russell AD. Principles of antimicrobial activity and resistance. In: Block SS, editor. Disinfection, sterilization and preservatives. Philadelphia: Lippincott Williams & Wilkins; 2001. p. 31–56.

Salim MM, Malek NANN. Characterization and antibacterial activity of silver exchanged regenerated NaY zeolite from surfactant-modified NaY zeolite. Mater Sci Eng C. 2016;59:70–7.

Santos MF, Oliveira CM, Tachinski CT, Fernandes MP, Pich CT, Angioletto E, et al. Bactericidal properties of bentonite treated with Ag^+ and acid. Int J Miner Process. 2011;100:51–3.

Shameli K, Ahmad MB, Zargar M, Wan Yunus WMZ, Rustaiyan A, Ibrahim NA. Synthesis of silver nanoparticles in montmorillonite and their antibacterial behavior. Int J Nanomedicine. 2011;6:581–90.

Shameli K, Ahmad MB, Al-Mulla EAJ, Shabanzadeh P, Bagheri S. Antibacterial effect of silver nanoparticles on talc composites. Res Chem Intermed. 2013;41(1):251–63.

Shvedova AA, Pietroiusti A, Fadeel B, Kagan VE. Mechanisms of carbon nanotube-induced toxicity: focus on oxidative stress. Toxicol Appl Pharmacol. 2012;261(2):121–33.

Sohrabnezhad S, Mehdipour Moghaddam MJ, Salavatiyan T. Synthesis and characterization of CuO-montmorillonite nanocomposite by thermal decomposition method and antibacterial activity of nanocomposite. Spectrochim Acta Pt A-Mol Biomol Spectr. 2014;125:73–8.

Sohrabnezhad S, Pourahmad A, Mehdipour Moghaddam MJ, Sadeghi A. Study of antibacterial activity of Ag and Ag_2CO_3 nanoparticles stabilized over montmorillonite. Spectroc Acta Pt A-Mol Biomol Spectr. 2015;136:1728–33.

Sondi I, Salopek-Sondi B. Silver nanoparticles as antimicrobial agent: a case study on *E. coli* as a model for Gram-negative bacteria. J Colloid Interface Sci. 2004;275:177–82.

Song J, Li Y, Hu CH. Effects of copper-exchanged montmorillonite, as alternative to antibiotic, on diarrhea, intestinal permeability and proinflammatory cytokine of weanling pigs. Appl Clay Sci. 2013;77-78:52–5.

Sui M, Zhang L, Sheng L, Huang S, She L. Synthesis of ZnO coated multi-walled carbon nanotubes and their antibacterial activities. Sci Total Environ. 2013;452-453:148–54.

Tang J, Chen Q, Xu L, Zhang S, Feng L, Cheng L, et al. Graphene oxide–silver nanocomposite as a highly effective antibacterial agent with species-specific mechanisms. ACS Appl Mater Interfaces. 2013;5(9):3867–74.

Tegos GP, Demidova TN, Arcila-Lopez D, Lee H, Wharton T, Gali H, et al. Cationic fullerenes are effective and selective antimicrobial photosensitizers. Chem Biol. 2005;12(10):1127–35.

Tekin R, Bac N. Antimicrobial behavior of ion-exchanged zeolite X containing fragrance. Microporous Mesoporous Mater. 2016;234:55–60.

Tong G, Yulong M, Peng G, Zirong X. Antibacterial effects of the cu(II)-exchanged montmorillonite on *Escherichia coli* K88 and *Salmonella choleraesius*. Vet Microbiol. 2005;105:113–22.

Top A, Ülkü S. Silver, zinc, and copper exchange in a Na-clinoptilolite and resulting effect on antibacterial activity. Appl Clay Sci. 2004;27:13–9.

Üreyen ME, Doğan A, Koparal AS. Antibacterial functionalization of cotton and polyester fabrics with a finishing agent based on silver-doped calcium phosphate powders. Text Res J. 2012;82(17):1731–42.

Valášková M, Martynkova GS. Vermiculite: structural properties and examples of the use, clay minerals in nature-their characterization, modification and application. InTech.; 2012. p. 326. ISBN 978-953-51-0738-5.

Valášková M, Hundáková M, Mamulová Kutláková K, Seidlerová J, Čapková P, Pazdziora E, et al. Preparation and characterization of antibacterial silver/vermiculites and silver/montmorillonites. Geochim Cosmochim Acta. 2010;74:6287–300.

Vargas-Reus MA, Memarzadeha K, Huang J, Renc GG, Allakera RP. Antimicrobial activity of nanoparticulate metal oxides against peri-implantitis pathogens. Int J Antimicrob Agents. 2012;40:135–9.

Vincent M, Hartemann P, Engels-Deutsch M. Antimicrobial applications of copper. Int J Hyg Environ Health. 2016;219:585–91.

Wang S, Peng Y. Natural zeolites as effective adsorbents in water and wastewater treatment. Chem Eng J. 2010;156:11–24.

Xia MS, Hu CH, Xu ZR. Effects of copper bearing montmorillonite on the growth performance, intestinal microflora and morphology of weanling pigs. Anim Feed Sci Technol. 2005;118:307–17.

Xiu ZM, Zhang QB, Puppala HL, Colvin VL, Alvarez PJJ. Negligible particle-specific antibacterial activity of silver nanoparticles. Nano Lett. 2012;12:4271–5.

Xu G, Qiao X, Qiu X, Chen J. Preparation and characterization of nano-silver loaded montmorillonite with strong antibacterial activity and slow release property. J Mater Sci Technol. 2011;27(8):685–90.

Yamamoto O, Sawai J, Sasamoto T. Activated carbon sphere with antibacterial characteristics. Mater Trans. 2002;43(5):1069–73.

Yang X, Ebrahimi A, Li J, Cui Q. Fullerene-biomolecule conjugates and their biomedicinal applications. Int J Nanomedicine. 2014;9:77–92.

Yuan W, Jiang G, Che J, Qi X, Xu R, Chang MW, et al. Deposition of silver nanoparticles on multiwalled carbon nanotubes grafted with hyperbranched poly(amidoamine) and their antimicrobial effects. J Phys Chem C. 2008;112:18754–9.

Zhang Y, Chen Y, Zhang H, Zhang B, Liu J. Potent antibacterial activity of a novel silver nanoparticle-halloysite nanotube nanocomposite powder. J Inorg Biochem. 2013;118:59–64.

Zhao D, Zhou J, Liu N. Preparation and characterization of Mingguang palygorskite supported with silver and copper for antibacterial behavior. Appl Clay Sci. 2006;33:161–70.

Zhou Y, Xia M, Ye Y, Hu C. Antimicrobial ability of Cu^{2+}-montmorillonite. Appl Clay Sci. 2004;27:215–8.